DEPARTMENT OF EARTH SCIENCES

DISTRIBUTION, MORPHOMETRY AND GENESIS OF DRUMLINS AND STREAMLINED TILL PATCHES IN SOUTHERN SWEDEN

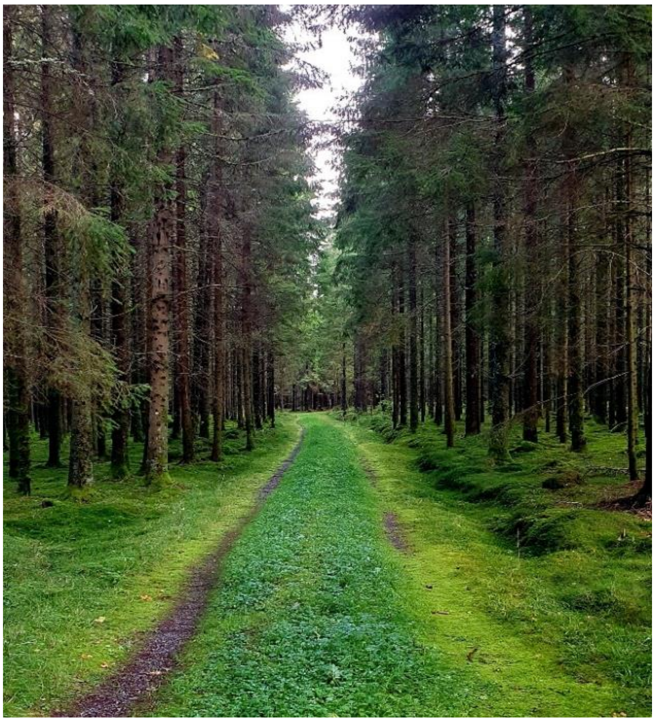

Christopher Pusterli

Degree project for Master of Science (120 hec) with a major in Earth Sciences
2024, 120 HEC
Second Cycle

Abstract

Research on streamlined landforms offers valuable insights into the evolution of glaciated landscapes and the characteristics of the ice sheets responsible for their formation. Despite the significance of these bedforms, the exact processes responsible for their subglacial formation remain a subject of debate. The goal with this master thesis is to identify and analyze drumlins and streamlined till patches in southern Sweden to enhance the understanding of their distribution, morphometrics and genesis. To answer the set goals, this study was carried out through GIS-, field-, and lab work. A total of 1187 drumlins and streamlined till patches were identified in this study, and they are mainly situated at elevated and/or eroded surface forms of the bedrock. Length, width, elongation ratio, area, spacing between features, height, and orientation were measured in this study for all the landforms, as well as drumlins and streamlined till patches separately. The length, width, and height of the drumlins are generally larger than other drumlins identified within Sweden and elsewhere. Only a few parameters show strong correlations with each other, namely length vs width, length vs area, and width vs area. Drilling and excavation data showed 78 features with diamicton all the way down to the bedrock. Nine landforms were identified with sorted sediment under a cover of diamicton, one from field work and eight from compilation of previous drillings and excavations. Sand was predominantly found here. The sorted sediment is interpreted to predate the overlying diamicton as it may have been deposited during a previous glaciation. 1083 of the mapped drumlins and streamlined till patches were furthermore found with bedrock knobs. This suggests that presence of bedrock had a significant role in the landform formation. Undulated hilly terrain is a key aspect in the formation of mapped drumlins and streamlined till patches, as it may control the accumulation and distribution of material. Multiple studies propose that drumlins can be classified according to three primary processes shaping their formation: erosion, deposition and deformation. The first two have been considered in this study. Evidence of erosion, such as the presence of older sub-till sediment, margins altered by meltwater corridors, the shielding effect of bedrock knobs, and the preservation of sediment, highlights potential mechanisms contributing to the formation of drumlins and streamlined till patches. Evidence of deposition are indicated through the presence of till comprising the mapped landforms. Presence of sorted sediment could also have induced the deposition of till, resulting in the emplacement of till on top of the sorted sediment.

Keywords: Drumlins, Streamlined till patches, Southern Sweden, LiDAR, Distribution, Morphometry, Landform genesis

Sammanfattning

Forskning om strömlinjeformade landformer har gett värdefulla insikter i utvecklingen av glaciala landskap och egenskaperna hos de inlandsisar som är ansvariga för deras bildande. Trots landformernas betydelse är de exakta processerna för hur de bildades dock inte helt klarlagda. Målet med den här masteruppsatsen är att identifiera och analysera drumliner och *Streamlined till patches* i södra Sverige i syfte att öka förståelsen för deras fördelning, morfometri och ursprung. För att besvara målen genomfördes GIS-, fält- och laboratoriearbete. Totalt identifierades 1187 drumliner och *Streamlined till patches* i den här studien och de är främst lokaliserade på upphöjda och/ eller eroderade ytor av berggrunden. Längd, bredd, längd-bredd-förhållande, area, avstånd mellan landformer, höjd och orientering har mätts för samtliga landformer, såväl som hos drumliner och *Streamlined till patches* separat. Drumlinernas längd, bredd och höjd är generellt sett större än andra drumliner som identifierats inom och utanför Sverige. Endast ett fåtal parametrar visar starka korrelationer med varandra, vilka är längd vs bredd, längd vs area samt bredd vs area. Tidigare markundersökningar (från borrning och maskingrävning) visade sammanlagt 78 landformer med morän ända ner till berggrunden. Nio landformer identifierades med sorterade sediment under lager av morän, en från fältarbete och åtta från sammanställning av tidigare borrningar och maskingrävningar. Sand hittades i huvudsak här. Det sorterade sedimentet tolkas vara äldre än det överliggande moränlagret eftersom det kan ha avsatts under en tidigare glaciation. 1083 av de kartlagda drumlinerna och *Streamlined till patches* hittades dessutom med berg i dagen. Detta indikerar att närvaron av berggrunden hade en betydande roll i bildandet av landformerna. Kuperad terräng är en nyckelaspekt i bildandet av de karterade drumlinerna och *Streamlined till patches,* eftersom den kan kontrollera ackumuleringen och fördelningen av material. Flertalet studier föreslår att drumliner kan klassificeras enligt tre primära processer under deras bildande: erosion, deponering och deformering. De två första har beaktats i denna studie. Bevis på erosion, såsom närvaron av äldre sediment under lager av morän, kanter formade av smältvattenkorridorer, skyddande effekten från berggrund och bevarandet av sediment, belyser potentiella mekanismer som bidrar till bildandet av de karterade landformerna. Tecken på deponering indikeras genom närvaron av morän i de karterade drumlinerna och *Streamlined till patches*. Närvaron av sorterat sediment skulle också kunna inducera avsättningen av morän, vilket resulterade i att morän placerades ovanpå det sorterade sedimentet.

Acknowledgments

First and foremost, I want to thank my two supervisors, Mark D. Johnson and Christian Öhrling, for their endless support and enthusiasm throughout this master thesis. Thank you Jakob Heyman, my examiner, for your feedback, which has enhanced the quality and clarity of this work. Thank you Hanna Tinnerholm for agreeing to be my opponent and for the feedback resulting in the improvement of my manuscript. To Helene and Johanna, who kept me company on my days in the field, your presence made the journey all the more rewarding. Thank you!

Lastly, I want to thank friends and family for all the encouragement, support and laughs along the way.

Table of Contents

1 Introduction

Studies of streamlined landforms provide valuable information and insight about the evolution of glaciated landscapes and the characteristics of the ice sheets that shaped them (e.g. Benn & Evans, 1996; Stokes et al., 2012). Despite the significance of these bedforms, the exact processes responsible for their subglacial formation remain a subject of debate (Dowling, 2016; Dowling et al., 2015; Sookhan et al., 2022). The broad range of features used to describe drumlins, with variations in internal sediments and external expressions, contributes to various theories about their formation (e.g. Dowling, 2016; Iverson et al., 2017; Spagnolo et al., 2010; Stokes et al., 2011). However, the availability of high-resolution LiDAR (Light detection and ranging) has reenergized the geomorphological scene as new light is shed on studies concerning landforms and landscape processes. The digital elevation data enables, for example, simplified interpretation of patterns within a population of landforms, uncover previously undiscovered connections among landforms and provide evidence either in favor of or against hypotheses regarding the genesis and development of landforms and landscapes (Napieralski & Nalepa, 2010).

1.1 General characteristics of glacially lineated landforms

1.1.1 Drumlins

A drumlin is a subglacial landform and can loosely be described as a smooth oval shaped hill, mostly composed of glacial till (Strahler & Strahler, 2004). With their general characteristics, drumlins exhibit a variety of shapes and forms (Clark et al., 2009). There is however no strict definition of the drumlin size, but they tend to show up to several kilometers in length (Clark et al., 2009), up to a few kilometers in width (Clark et al., 2009) and up to 50 m in height (TUOS, 2024a). Despite that many drumlins have been identified with a rock core in southern Sweden (e.g. Dowling et al., 2015), they'll in this study simply be called "drumlins".

Examples of drumlins in southern Sweden are illustrated in figure 1, where 1.D and F are identified as such. Bedrock knobs have also been marked out within and at the margins of the drumlins illustrated in figure 1 as many drumlins are associated with these.

1.1.2 Streamlined till patches

Another landform found within the southern Swedish streamlined terrain has been described as patches of streamlined till (as identified by for example Dowling, 2016 and Möller & Dowling, 2018), which in this study are referred to as a streamlined till patch. These features are hence, as the name suggests, characterized by its streamlined surface cover of till.

Figure 1 shows various types of streamlined till patches in southern Sweden, with 1.A, B, C, and E identified as such. Bedrock knobs have also been marked out within and at the margins of these landforms.

However, in other studies (e.g. Dowling, 2016; Dowling et al., 2015), streamlined till patches have instead been mapped as a group of drumlins rather than a singular landform. In this study however, this feature will be viewed as the latter.

1.1.3 Difference between drumlins and streamlined till patches

The difference between drumlins and streamlined till patches lies in their respective size. Streamlined till patch is generally larger in both length and width and has generally a smaller elongation ratio compared to drumlins.

As exemplified in figure 1, the streamlined till patches (1.A, B, C and E) show a notably larger size compared to the drumlins (1.D and F), as well as not being as elongated.

1.1.4 Other streamlined landforms

Crag & tails are a common subglacial landform characterized by a “tail” of sediment sited at the lee side of bedrock (crag). The tail is pointing in a down-ice direction (TUOS, 2024b). Despite these landforms being common features associated with drumlins and can sometimes be present on other streamlined landforms (figure 1A, D and F), crag and tails are not considered in this study. Further, landforms defined by a narrow and elongated form, such as flutes (Ely et al., 2016) and mega-scale glacial lineations (Sookhan et al., 2022), will neither be discussed.

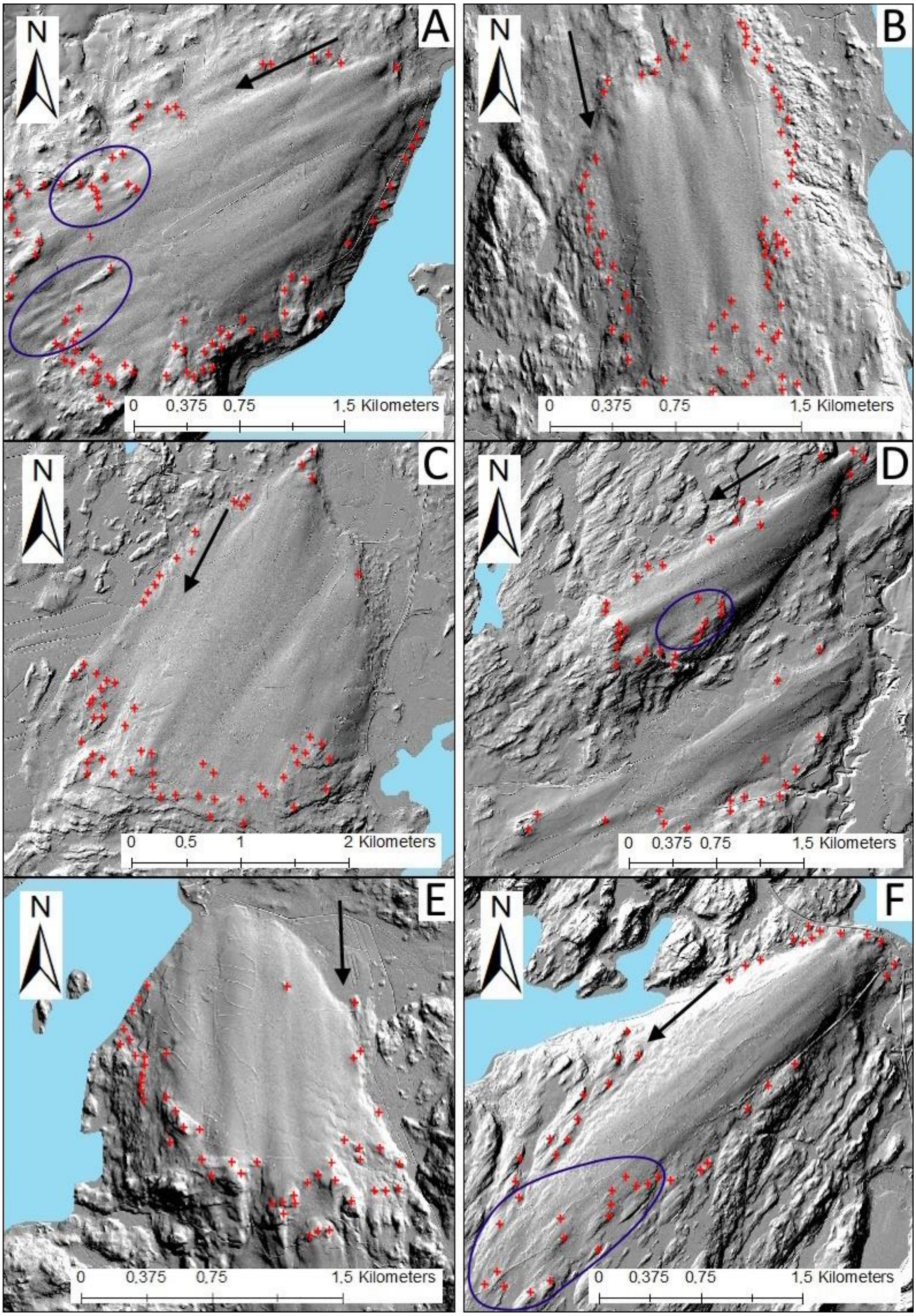

Figure 1. Examples of drumlins and streamlined till patches in southern Sweden, illustrating variations in size and shape. A, B, C and E shows streamlined till patches, whereas D and F shows drumlins. The black arrows show the direction of the ice, the red plus signs (+) marks bedrock knobs within and at the margins of the landforms and the dark purple markings show areas with crag & tails. Data: © Lantmäteriet Elevation Data.

1.2 Lidmoräner vs Drumlins and Streamlined Till Patches

1.2.1 Definition of a *Lidmorän*

In both earlier and more recent Swedish literature, notably in publications by The Geological Survey of Sweden (SGU), landforms that herein are called *drumlins and streamlined till patches* have often been referred to as a "Lidmorän" (English: Lid= Slope, morän= moraine). They're described by Gillberg (1976) (referred to as Lid Moraines) in an extensive study carried out in southern Sweden as large streamlined till accumulations without a ridge form. Their margin can sometimes successively integrate with the surrounding terrain (Gillberg, 1976). Påsse (1988) has, in southwestern Sweden (SE Varberg/ SW Ullared), used the term "lidmoräner" (plural form) as those without an oval contour-line crest top (as often seen on drumlins), but instead with slightly arched slopes that lie parallel to the ice movement, most distinctly at the stoss-side of the elevated bedrock knobs. Fredén (1983) emphasizes that the lack of a marked crest stands out as the most distinctive feature of the landform. Furthermore, Påsse (1988) suggests that lidmoräner and drumlins may have been formed in the same way, although the difference between which landform is which is assumed to lie in the shape of the stoss side of the bedrock. The author posits that Lidmoräner have formed at larger elevated areas compared to drumlins (Påsse, 1988). Fredén (1983) highlights that their formation is mainly bedrock dependent. Also, Gillberg (1976) emphasizes that the accumulation of till can (locally) extend over the topographic bedrock highs, and cover most of the bedrock. However, this is contingent upon the bedrock knob not being excessively large.

The term "Lidmorän" has not been widely used in the literature and the definitions found are too imprecise and inconsistent. There is also no commonly used English word to describe these landforms, where the term "Lid Moraine" (as used by Gillberg, 1976) is only sparingly used in literature. Therefore, the descriptive terms "Drumlins and Streamlined till patches" will be used in this study. The landforms included in these terms could hence be referred to as Lidmoräner. By following the definition of a Lidmorän as described above, the landforms correspond in many ways with Drumlins and Streamlined till patches. However, the definition of a Lidmorän given above is not enough to determine a complete overlap.

1.2.2 Characteristics of a *Lidmorän*

Despite that the morphometrics of the *Lidmoräner* are sparingly investigated in literature, Vikberg-Samuelsson et al. (2022) have made approximate measurements of their size, concluding a length between 1-4 km, width around 1 km and a height between 10-30 m.

Lidmoräner have according to Vikberg-Samuelsson et al. (2022) furthermore been observed with a sorted sediment core. Documentation of till-capped sorted sediment extends back to the 19th century, with studies conducted by for example Fredholm (1875). The reason Vikberg-Samuelsson et al. (2022) investigated these *lidmoräner* was to determine whether there are geological formations in an area north of Växjö, in addition to typical glacial river deposits and delta formations, which could constitute significant groundwater reservoirs. Sorted sediment within these landforms can hence contribute to a source of groundwater (Vikberg-Samuelsson et al., 2022).

1.2.3 Other terms used of a *Lidmorän*

Previous studies have described landforms corresponding to descriptions given for *lidmoräner*, as described above, but where other terms have been used. Studies like Ising (2012) and Bergström et al. (2019) have called these landforms "Moränlider", based on the *Lid Moraines* used by Gillberg (1976). This term has been used long before the study by Gillberg was published (e.g. Tamm, 1925, 1931; Statens Meteorologisk-Hydrografiska Anstalt, 1928) but where the term instead referred to a (often wooded) till-covered hillside (SAOB, 2024). Gillberg (1955) previously labeled the *Lid Moraines* as stoss-side moraines, but later revised his classification as they also can occur distally and extend over entire plateaus. In similarities to the initial term, Hillefors (1974) has described the landforms as toe cap-like stoss side drumlins due to their marginal form. Lidmoräner have moreover been analyzed in more recent studies but have been named under broader terms like drumlins and streamlined terrain (e.g. Dowling, 2016; Dowling et al., 2015; Möller & Dowling, 2016; Möller & Murray, 2015; Möller et al., 2020).

1.3 Major project goals

The goal with this master thesis is to identify, map and analyze drumlins and streamlined till patches in order to enhance the understanding of how these landforms are distributed across southern Sweden and to get insight about how they were formed.

1.3.1 Research questions

- How are the drumlins and streamlined till patches distributed across Southern Sweden?
- How does the morphometry differ within the mapped landforms, and other drumlinoid landforms?
- Are there local conditions (topography, bedrock, pre-existing sediment, etc.) that have influenced their distribution?
- How were these landforms formed and why do they have the distribution they have?

1.4 Background

1.4.1 Quaternary geological development in Scandinavia

The surficial deposits and landforms in Scandinavia owe their genesis primarily to the last ice age (Strahler & Strahler, 2004), spanning from approximately 115 000 years ago until the disappearance of the last remnants of the ice sheet, from the Scandinavian Mountains, probably around 9 500 years ago (Andrén et al., 2011; Regnéll et al., 2019).

During the last ice age, Scandinavia experienced successive advances of the ice sheet, each followed by a deglaciation. The two most extensive colder periods are called MIS 4 and

MIS 2 and occurred 71 000–57 000 years ago and 29 000–14 000 years ago respectively (Cohen & Gibbard, 2011). The relatively warmer period in between MIS 4 and MIS 2 is called MIS 3, which occurred 57 000-29 000 years ago (Cohen & Gibbard, 2011). During the cold period of MIS 4, the ice reached all the way down to Denmark (Houmark-Nielsen 2010; Möller et al., 2020). At a later stage, during the warmer period of MIS 3, the ice sheet eventually retreated up to the Scandinavian Mountain range (Houmark-Nielsen, 2010; Kleman et al., 2021). Around 35 000 years ago, the ice sheet advanced southward, reaching Denmark around 30 000 years ago, and eventually reached its maximum extent in Germany and Poland around 21 000 years ago (Hughes et al., 2016; Stroeven et al., 2016). Subsequently the ice retreated from its maximum, successively leaving northern Europe ice free. During this deglaciation, shorter cold periods occurred, including the Younger Dryas cold event between 12 800 and 11 700 years ago (Mangerud, 2021; Stroeven et al., 2016).

As the ice sheet advanced, loose material and rock fragments were transported and subsequently deposited directly from the ice, both beneath and in the frontal zone of the ice sheet. All types of material were transported and deposited, from clay to big boulders. Till, the most common sediment type in Sweden, originates from these processes. Conversely, during periods of glacial retreat and ice melting, deposition of more well-sorted sediments occurred, comprising materials such as gravel, sand, silt, and clay (Karlsson et al., 2021). Large volumes of meltwater were formed from the melting ice, giving rise to meltwater streams that eroded and transported materials while moving through tunnels within or beneath the ice. As the streams approached the ice margin, the speed of the meltwater decreased and larger material such as gravel and sand sank to the ground and accumulated. Finer material, namely silt and clay, was however transported further away from the ice margin and settled in quiet waters where the absence of turbulent waves and currents allowed for their deposition (Karlsson et al., 2021; SGU, 2020a).
Deposition of materials, as a result of fluctuations in the ice sheet marked by both advances and retreats, have had a great impact on the landscape, and consequently the surficial deposits and landforms (Karlsson et al., 2021). In places, these fluctuations have left distinct stratigraphic sequences composed of several layers of till, outwash and finer sediment.

1.5 Study area

The area of investigation covers southern Sweden (figure 2) and is limited by the southern border of the Norrland Terrain, a hilly terrain type characterized by hilltops ranging normally from 50 to 200 meters, with some reaching heights of up to 400 meters (Lidmar-Bergström, 2009). The Norrland Terrain was chosen as it acts like a natural border within the landscape, as it adjoins terrain with less relief differences.

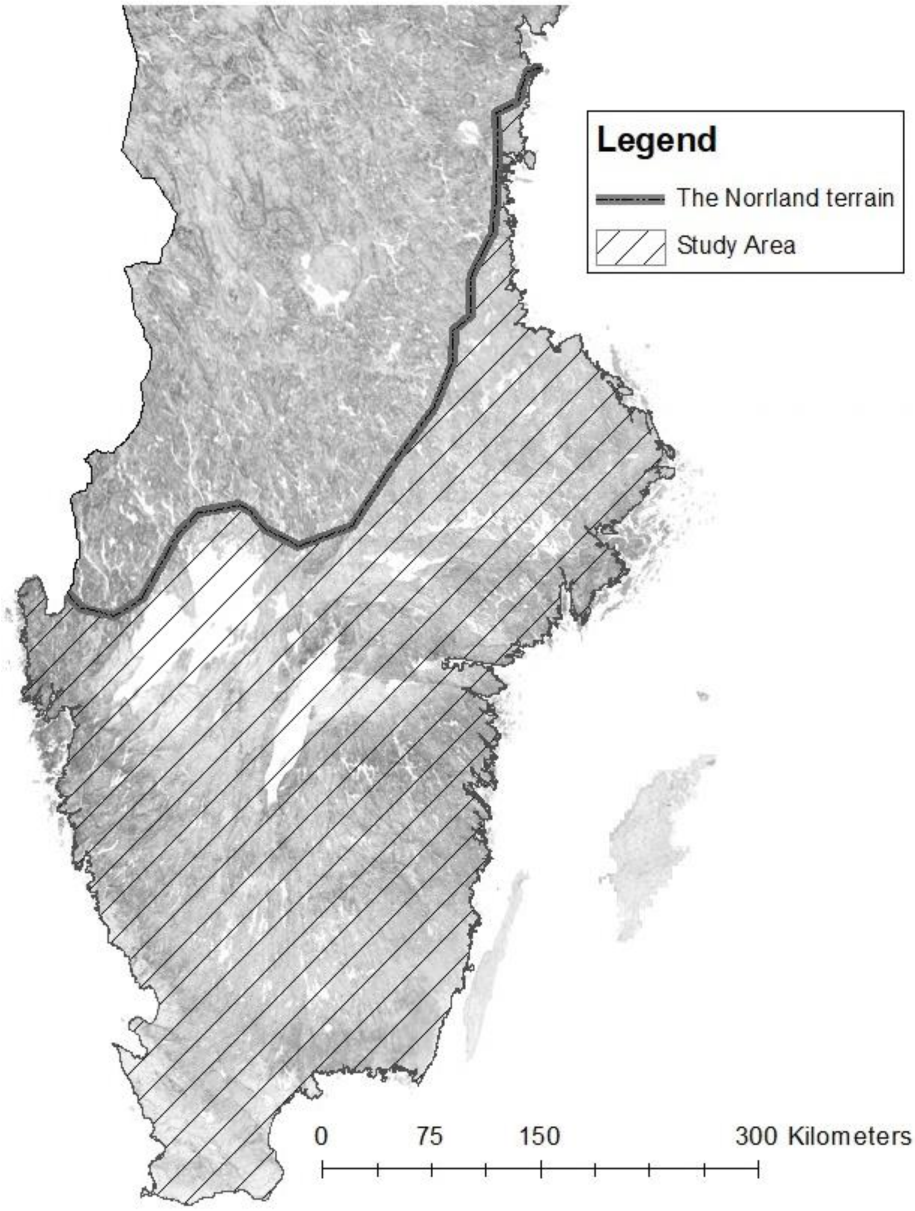

Figure 2. The study area is situated in southern Sweden, delineated by the southern border of the Norrland terrain. The Swedish archipelago is not included in this study, as well as Öland and Gotland. The hillshade in the background illustrates the topographic differences in the landscape. Data: © Lantmäteriet Height Model.

1.5.1 Regional overview

Southern Sweden showcases a diverse landscape characterized by various types of terrains. The Central Swedish Lowland, a region of relatively low relief and elevation, extends in a broad west-east trending belt roughly between the northern Götaland and the coast of Svealand (Lidmar-Bergström, 2009; VISS, 2023). Much of this area is coated by the uncovered sub-Cambrian peneplain (Green et al., 2013), which has emerged from beneath the Cambrian cover rock (Nordenskjöld, 1944). As the Cambrian rock eroded, it protected the Sub-Cambrian peneplain, which could have contributed to the shape it has today (Lidmar-Bergström et al., 2017). As documented by Rudberg (1960), the relative relief is less than 20 meters in well-preserved parts. Bedrock hills do however exist on the peneplain, but they are infrequent exceptions (Lidmar-Bergström, 1988). The same peneplain is also present on the east coast of Götaland (Lidmar-Bergström, 2009).

At the west and southern coasts of Götaland, a relatively hilly terrain is present, namely the Sub-Mesozoic hilly relief (figure 3). In southwestern Sweden, the surfaces of this terrain type emerge from Jurassic and Cretaceous rock covers. The topography is locally deeply kaolinized and is characterized by uneven topography, featuring glacially truncated tors, boulders composed of basement rocks, and an abundance of Jurassic and Cretaceous outliers (Lidmar-Bergström, 1988).

The South Swedish Upland, a geographic area that mainly covers central Götaland, is defined by its undulating hilly landscape (Lidmar-Bergström, 2009).
The South Swedish Dome, making up the South Swedish Upland (Lidmar-Bergström et al., 2017), emerges from sub-Cambrian cover rocks in the north and east and sub-Mesozoic cover rocks in the south and west (Green et al, 2013). In the Mesozoic Era, the region experienced a warm and humid climate, leading to substantial weathering of exposed bedrock. Subsequently, in the late Oligocene and early Miocene Epochs, the area underwent uplift, giving rise to the southern Swedish Dome (Lidmar-Bergström & Näslund, 2002). Much of the area lies from 200 m a.s.l., and the highest point, Tomtabacken, reaches 377 m a.s.l. Many residual hills are also situated at areas over 200 m a.s.l. (Lidmar-Bergström et al., 2017).
During the Neogene, the area experienced another uplift, accompanied by tilting and erosion. This geological event gave rise to the south Småland peneplain (Olvmo et al., 2005). The area lies mainly between 125-175 m a.s.l., where only a few residual hills are present (Lidmar-Bergström et al., 2017).

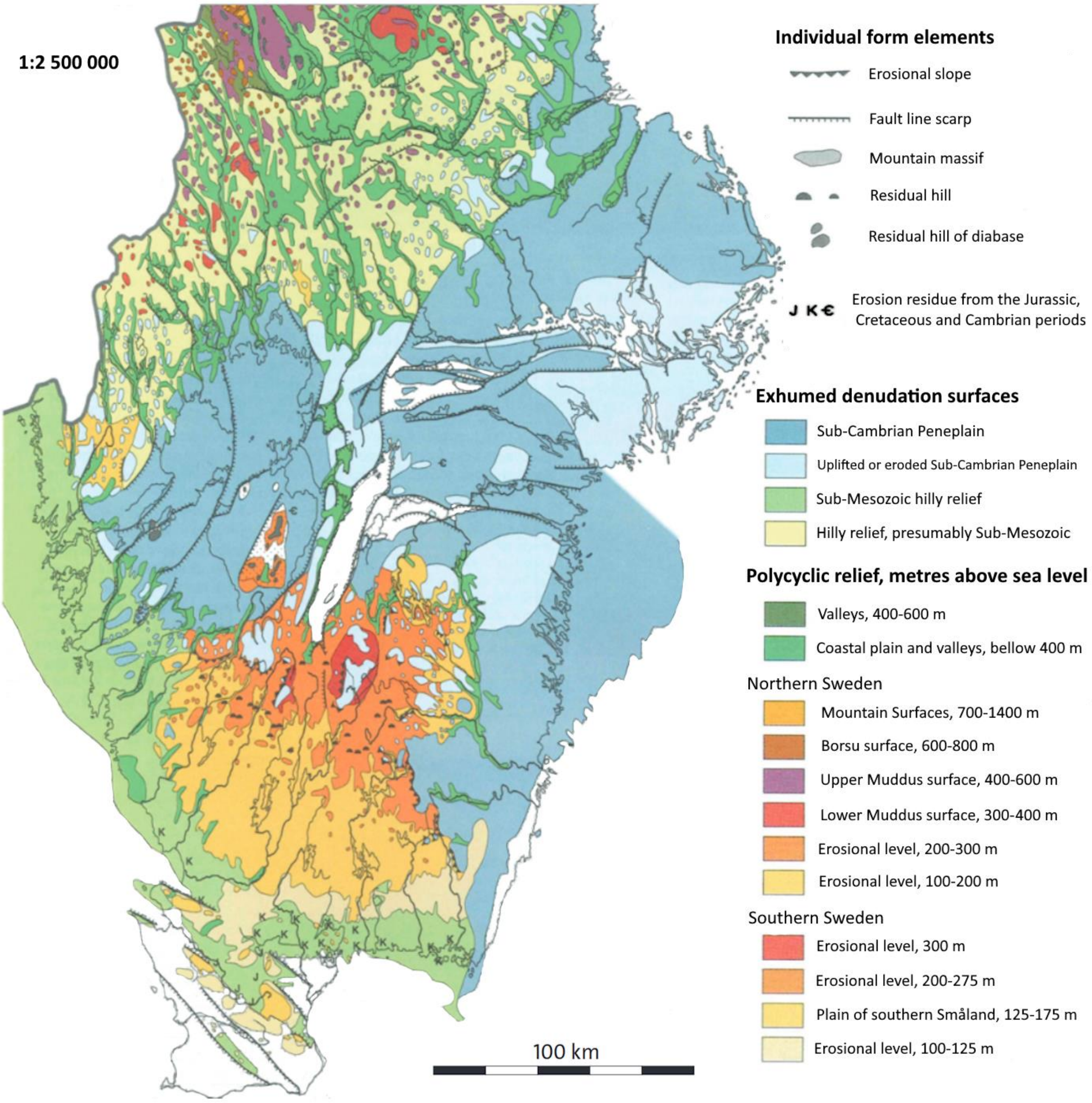

Figure 3. The surface shape of the bedrock in southern and central Sweden. Individual form elements and erosion residues are also marked out. Modified from Lidmar-Bergström (2009).

1.5.2 Previous investigations on drumlins and streamlines till patches in southern Sweden

The combined terms of drumlins and streamlined till patches have been documented across various regions within the study area, primarily through investigations conducted by the Geological Survey of Sweden (SGU). These regions include **Halland** (Påsse, 1993), **Småland** (Ising, 2012; Möller & Murray, 2015; Möller et al., 2020; Sundevall, 2006; Svantesson, 2001; Vikberg-Samuelsson et al., 2022), **Dalsland** (Hilldén, 2008), **Västergötland** (Hilldén, 1984, 1992; Hilldén & Sundevall, 2010) and **Skåne** (Ising et al., 2019). It should however be noted that these studies, while valuable in their localized identifications, do not provide a comprehensive analysis of the distribution across the regions.

2 Method

To answer the set goals and research questions, this study has been carried out through GIS-, field-, and lab work. Within the GIS-work, drumlins and streamlined till patches were mapped, and morphometrics (length, width, elongation ratio, area, spacing between features, height and orientation) were measured. Correlation analysis was conducted on the measured morphometrics. Data from previous drilling and excavations (from SGU) was compiled, and any bedrock knob exposed within and at the margins of the mapped landforms was marked.
Field work was carried out in southwestern Sweden, investigating material found within selected landforms. This includes insight about any sub-till sediment present. Classification of the deposits was made in the field. However, samples were collected in cases where uncertainties lied in the classification. These samples were investigated further in the lab, in order to determine their grain size distribution. Dry sieve and hydrometer analysis were conducted.

The GIS work was conducted from September to December 2023, while the fieldwork took place sporadically in October of the same year. Subsequent lab work was carried out in November 2023.

2.1 GIS mapping and analysis

2.1.1 Data acquisition and preparation

The area of investigation was manually mapped, utilizing the Swedish national height model (*Nationella höjdmodellen*), which is a Digital Elevation Model (DEM) derived from LiDAR data. The data acquired came with a cell size of 2 meters, an average height accuracy of 0.1 meters and a horizontal accuracy of 0.3 meters (Lantmäteriet, 2020). Elevation data (grid 2+), General Map (Översiktskartan), Orthophoto, Quaternary deposits and Stratigraphic sequences were used for mapping, analysis and visualization, and were acquired from the *Geodata Extraction Tool* (GET), the download service from *Swedish University of Agricultural Sciences* (SLU) (SLU, 2024). The three first products mentioned are offered by Lantmäteriet (Lantmäteriet, 2024), whereas the two last ones are provided by SGU (SGU, 2019). The limit of the highest shoreline, also used for analysis and visualization, was acquired from SGU (ibid).

2.1.2 Mapping procedure

ESRI ArcMap 10.8.1 was used for the mapping. To interpret landforms within the landscape, hillshades of illumination azimuth 315° and 45° were used to ensure unbiased mapping of features with varying orientations. The study area was mapped twice to make sure all drumlins and streamlined till patches were marked. The area was mainly screened at scales between 1:80 000-1:100 000, but 1:20 000 was also used when more precise interpretation was required. Drumlins and streamlined till patches were marked with a polygon.

To ensure objectivity in the mapping process, the landforms investigated in this study were defined early on. This encompasses large streamlined till accumulations and should be distinguishable in the landscape. Features should hence stand out from the surrounding landscape in both the A and B axes. Their margins could however successively integrate with the terrain around. These landforms could also show slightly arched slopes that lie parallel to the ice movement, as well as presence of bedrock knobs within or at the margin of the landforms. The landforms mapped in this study would hence correspond to the descriptions of Lidmoräner as described in Swedish literature.

2.1.3 Approach to obtain morphometrics

The following parameters were measured to define the morphometry of the landforms: length, width, elongation ratio, area, spacing, height and orientation.

Length and width were calculated using the “Minimum Bounding Geometry”, a tool offered in ArcMap. As landforms were marked with polygons, “Convex Hull” (the smallest convex polygon enclosing the feature) was chosen as the geometry type, being the sole option for polygon representation. This ensured that the output geometry followed the original feature shape to a significant extent. The Minimum Bounding Geometry tool gave, in a few cases, wrong values if the polygon had a too rounded or too irregular form. Landforms with a greater width than length were also given incorrect values as the tool measured the longest distance between any two vertices of the polygon as **length**, and thus the shortest distance as **width** (ESRI, 2024). All incorrect values were manually adjusted. The A-axis of these landforms was drawn to align with the direction of the ice, which could be observed on their streamlined surface. The B-axis was instead set roughly perpendicular to this direction.

The orientation was also calculated using the “Minimum Bounding Geometry”-tool, but “Rectangle By Area” was instead used as the geometry type rather than “Convex Hull”-type, which tended to give incorrect values due to the general irregularities of the landforms. Despite this, a few fell out as they gave incorrect values. These were adjusted manually using the same approach used to correct the inaccurate values for length and width.

Measurements of the spacing between features was made using the “Near”-tool offered in ArcMap. The spacing was calculated between all the mapped features, as well as drumlins and streamlined till patches respectively.

When calculating the height of the features, the method by Spangolo et al. (2012) was used. This involved the following steps: (i) removing the features from the landscape; (ii) interpolating the “landform-less” area with surrounding landscape (named the “drumlin base”), as if the landforms been sliced off from the landscape; (iii) subtracting the elevation values from the “landform-less” DEM with the original DEM, resulting in a DEM where only the mapped landforms have elevation values; (iv) calculate the relief of the landforms using $h = a * \sin(90 - \theta)$, where **h** is the relief, **a** is the largest vertical length between the base and the surface of the landform, **θ** is the slope angle of the apparent base of the landform.
This formula is used for landforms lying on a base of any slope value, which includes all of this dataset. Landforms lying on a perfectly horizontal surface would only have to use the **a**-value to receive its relief. The data was subsequently exported to Excel, sorted for enhanced clarity, and then analyzed.

Like Spanolo et al. (2012), negative elevation values were encountered for some of the landforms. This phenomenon arises because, at the local level, a landform may feature either artificial or natural excavations resulting from erosion, such as a road cut, quarry, river incision, landslide, and more. When these excavations fall below the conceptual base of the landform, it gives rise to the presence of negative pixels (Spagnolo et al., 2012). Following their method, features with >25% negative pixel values were excluded from the height calculation, which was a total of 239 landforms (of 1176 in total).

2.1.4 Correlation analysis of morphometry

Statistical relationships between measured parameters including length, width, elongation ratio, area, spacing, and height were investigated using the Pearson correlation coefficient. Excel was utilized for this analysis.

Pearson correlation coefficient is a measurement of the linear relationship between two variables. It quantifies the degree to which two variables are related to each other. The correlation coefficient ranges from 1 to -1, where 1 indicates a perfect positive linear relationship, -1 a perfect negative linear relationship and 0 indicates no linear relationship between the variables (Newcastle University, 2024a).
In other words, the sign of the correlation coefficient (+ or -) indicates the direction of the relationship, while the magnitude (0 to 1) indicates the strength of the relationship (Newcastle University, 2024a).

To determine if the respective relation is statistically significant, a *p*-value was calculated using the “Regression-tool” in Excel (found in Data-> Data Analysis). If the *p*-value was lower than the set significance level (α) of 0.05, the relationship is statistically significant. The value of 0.05 was used as it’s a common choice in statistical tests (Newcastle University, 2024b). Statistical significance refers to the likelihood that a relationship between two or more variables is not due to chance, like random fluctuations or sampling error (University of Kentucky, 2024).

2.1.5 Approach to obtain information about sediment composition and stratigraphy of landforms

The sediment composition and stratigraphy of the mapped drumlins and streamlined till patches was characterized from published drill holes as well as some published excavation reports. This included information about any sub-till sediment. The data are based on observations from previous mapping from SGU, as well as geotechnical investigations carried out by other actors such as municipalities, Swedish Transport Administration (Trafikverket), Swedish Fortifications Agency (Fortifikationsverket) and consultants. It should however be noted that the accuracy of this data can at times vary, where errors and incomplete data may occur (SGU, 2024a). Drill hole/ excavation data situated within landforms were given the respective ID of the landform in ArcGIS. Those outside any landform were removed. Subsequently, the data was exported to Excel, sorted for enhanced clarity, and then analyzed. Data irrelevant for this study, including unspecified material and insufficient observations, were filtered out.

2.1.6 Bedrock knobs

Exposed bedrock knobs have been marked for each of the mapped landforms using LiDAR and Orthophotos. The Quaternary deposits map provided by SGU was also used to facilitate the identification as exposed bedrock is displayed as a layer. In cases when uncertain, no bedrock knob was marked.

2.1.7 Data visualizations

ArcMap, Excel and Paint.NET (Paint.NET, 2024) were mainly used for illustrating the collected data, with maps, tables and charts.

2.2 Field Work

The field work was carried out in southwestern Sweden and 13 sites were visited (figure 4). This included 12 different landforms (five drumlins and seven streamlined till patches), where only sites 11 & 12 were located within the same feature. As the goal of the field work was to get insight about the material within the features, old excavation/pit sites, cuts and other depressions in the ground were investigated. The sites were also chosen as they were easy to get to and somewhat close to Gothenburg.

Drilling/ excavation would be the most appropriate method when investigating the material within drumlins and streamlined till patches. However, machines necessary to carry out that type of method were not available in this thesis. Therefore, for each site, a shovel and an auger were used in the investigation to get an insight about the sediment. The coordinates for each site are located in appendix 1.

Investigations of the material were conducted at each site using shovel and handheld auger, both horizontally into the cut, as well as downwards at the base of the site. These procedures were conducted to a depth of approximately 1 meter or until the material made it hard to continue. Additionally, the top meter of the outcrop was examined. The number of boulders at the surface was also observed.

Sediment composition and type was determined in the field, and samples were collected at sites where classification was uncertain. Each sample was put into a plastic bag and marked with the location it was taken at, and later taken to the lab.

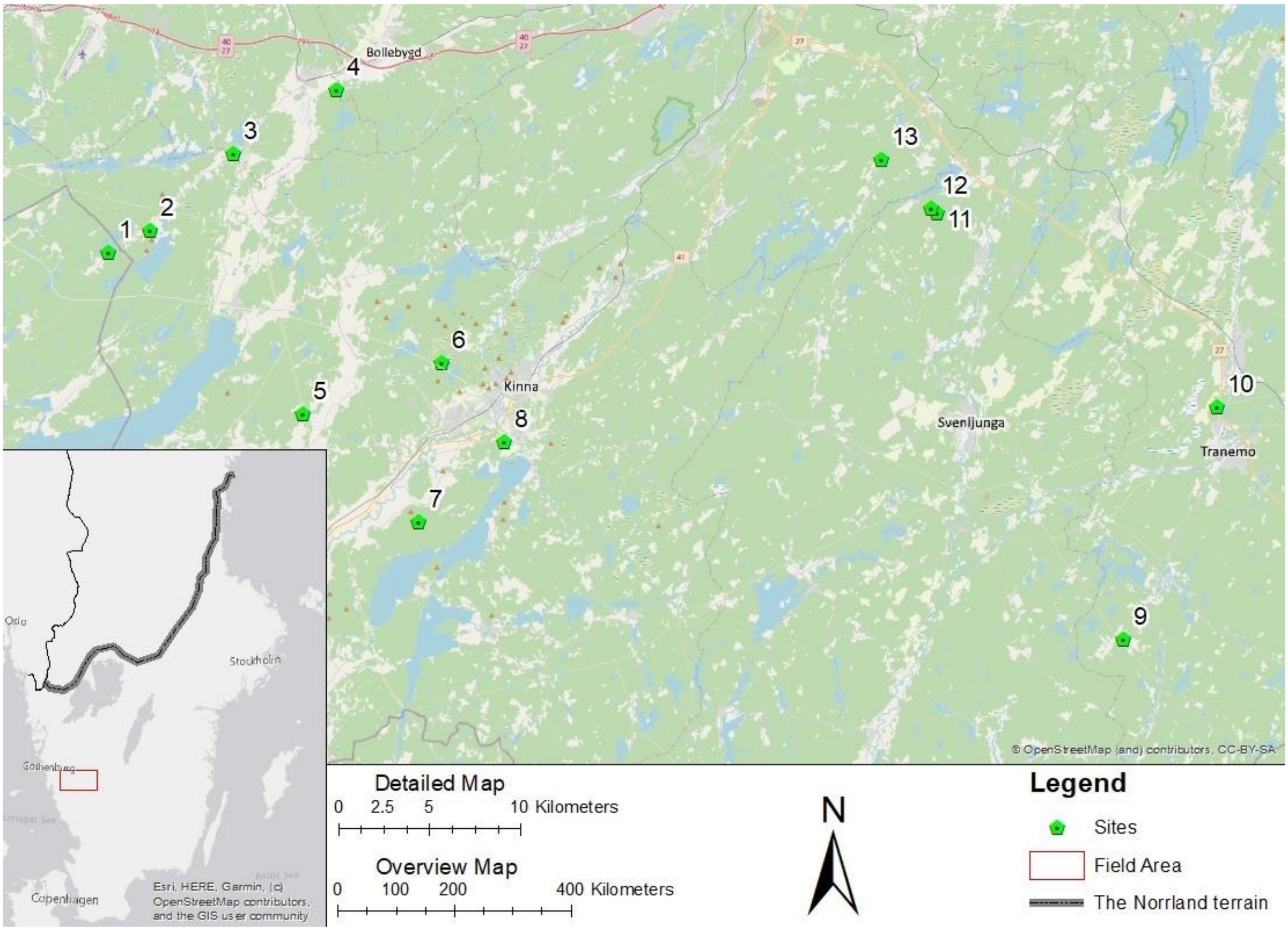

Figure 4. Map over the area the field work was carried out. The smaller map on the left side shows an overview of South and Central Sweden, with the field area marked. The larger, more detailed map shows the visited sites, a total of 13. Site 1, 2, 3, 5 and 6 are located on drumlins and site 4, 7, 8, 9, 10, 11, 12 and 13 on streamlined till patches. The southern border of the Norrlands terrain is marked out on the overview map. Data: © OpenStreetMap, contributors, CC-BY-SA and the GIS user community.

2.3 Lab Work

The grain size of the eight collected samples was measured with standard sieve- and hydrometer technique. Each sample underwent appropriate preparation procedures prior to the measurements.

2.3.1 Lab preparations

The eight collected samples, which were approximately 1 kg each, were initially air dried for at least one week depending on when it was collected from the field.
Organic material was removed from each sample by hand, as well as particles larger than 16 mm, using a 16 mm sieve. 500 g of each sample was used for the sieve analysis, and 100 g for the hydrometer analysis.

2.3.2 Grain-size analysis

By combining the sieve- and hydrometer techniques, the distribution of particles above, as well as below 0.063 mm could be determined. The sieve analysis was used to determine coarser particles within the sand and gravel spectrum (>0.063 mm; after the grain size scale standard by ISO, 2017), and the hydrometer analysis to determine the particles within the silt and clay spectrum (<0.063 mm) (López, 2016). The sieve analysis was conducted over the course of two days, whereas the hydrometer analysis took four days to complete. The latter was conducted in two separate sessions, analyzing half of the samples each time. Protocols for the sieve- and hydrometer analysis were used throughout the analyses to record various measurements. These are found in appendixes 2 and 3. Blow-by-blow descriptions of the sieve- and hydrometer analysis are moreover found in appendix 4.

2.3.3 Classification of sediment

The sediments have been classified according to ISO 14688-1:2017, *Identification and classification of soil*. Material comprising a diverse array of grain sizes (ISO, 2017) are defined as diamicton, and material dominated by one fraction was given that specific name (e.g. sand, gravel). Adjectives have been given in cases where any fractions are significant (e.g. sandy, sandy-silty), but not dominant.

3 Results

This section presents the outcomes derived from GIS analyses, field surveys, and laboratory investigations. The GIS work covers the distribution and classification of the mapped drumlins and streamlined till patches, including morphometry analysis, correlation analysis, compilation of previous drilling and excavation data and mapping of bedrock knobs found on mapped features. Furthermore, descriptions of visited field sites and the results of the grain size analysis are also presented.

3.1 Distribution and classification of drumlins and streamlined till patches

3.1.1 Distribution

A total of 1187 drumlins and streamlined till patches have been identified within the study area. Of these are 1037 features located above the highest shoreline (figure 5).

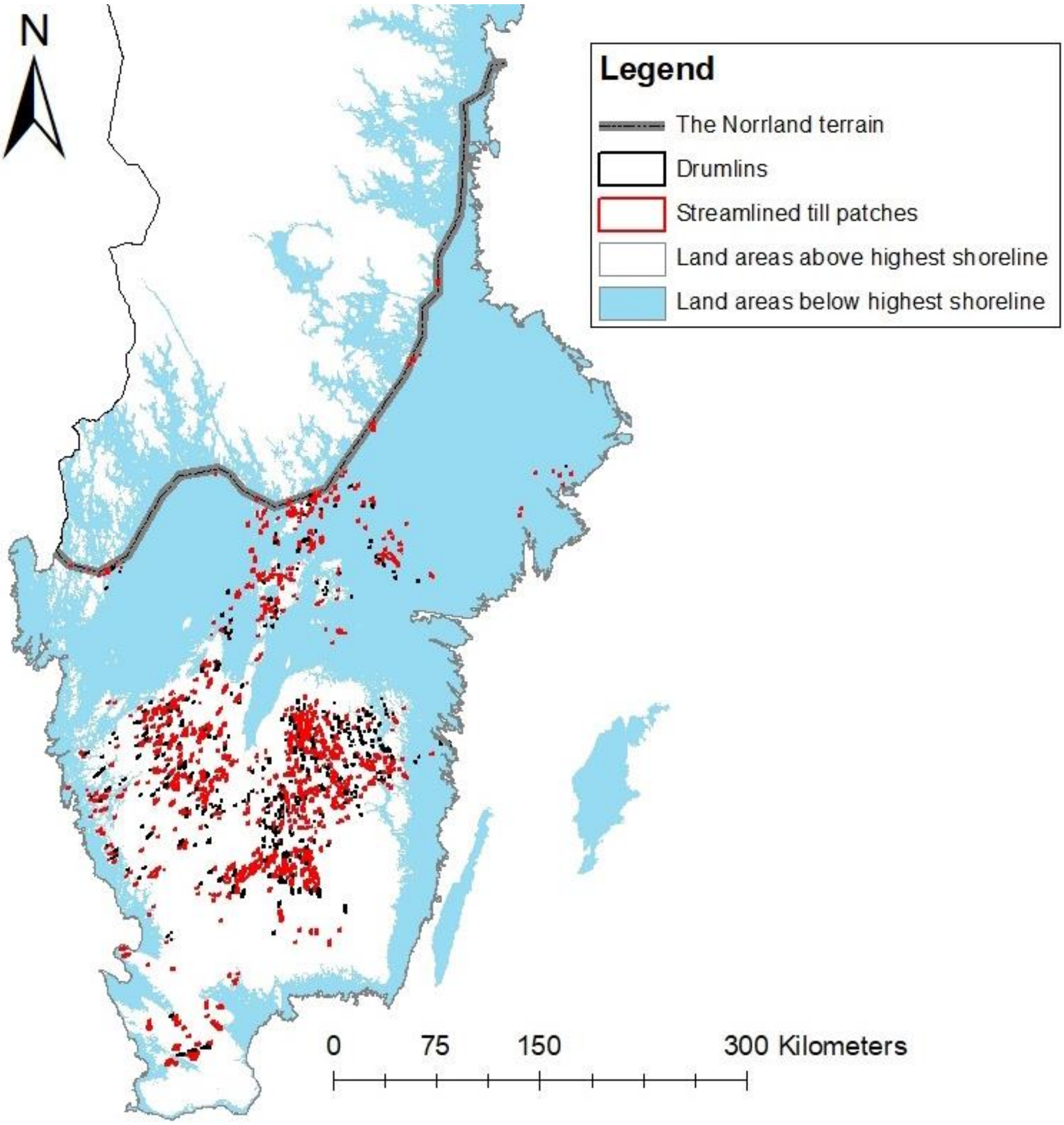

Figure 5. The distribution of the mapped drumlins and streamlined till patches. Land areas above and below the highest shoreline are visualized, as well as the southern border of the Norrland terrain. Data: © SGU Highest Shoreline, © Lantmäteriet General Map.

3.1.1.1 Detailed views of drumlins and streamlined till patches

Two detailed views of areas with drumlins and streamlined till patches within the study area are presented in figure 6. This exemplifies how the landforms are mapped, as the outline of respective feature are illustrated.

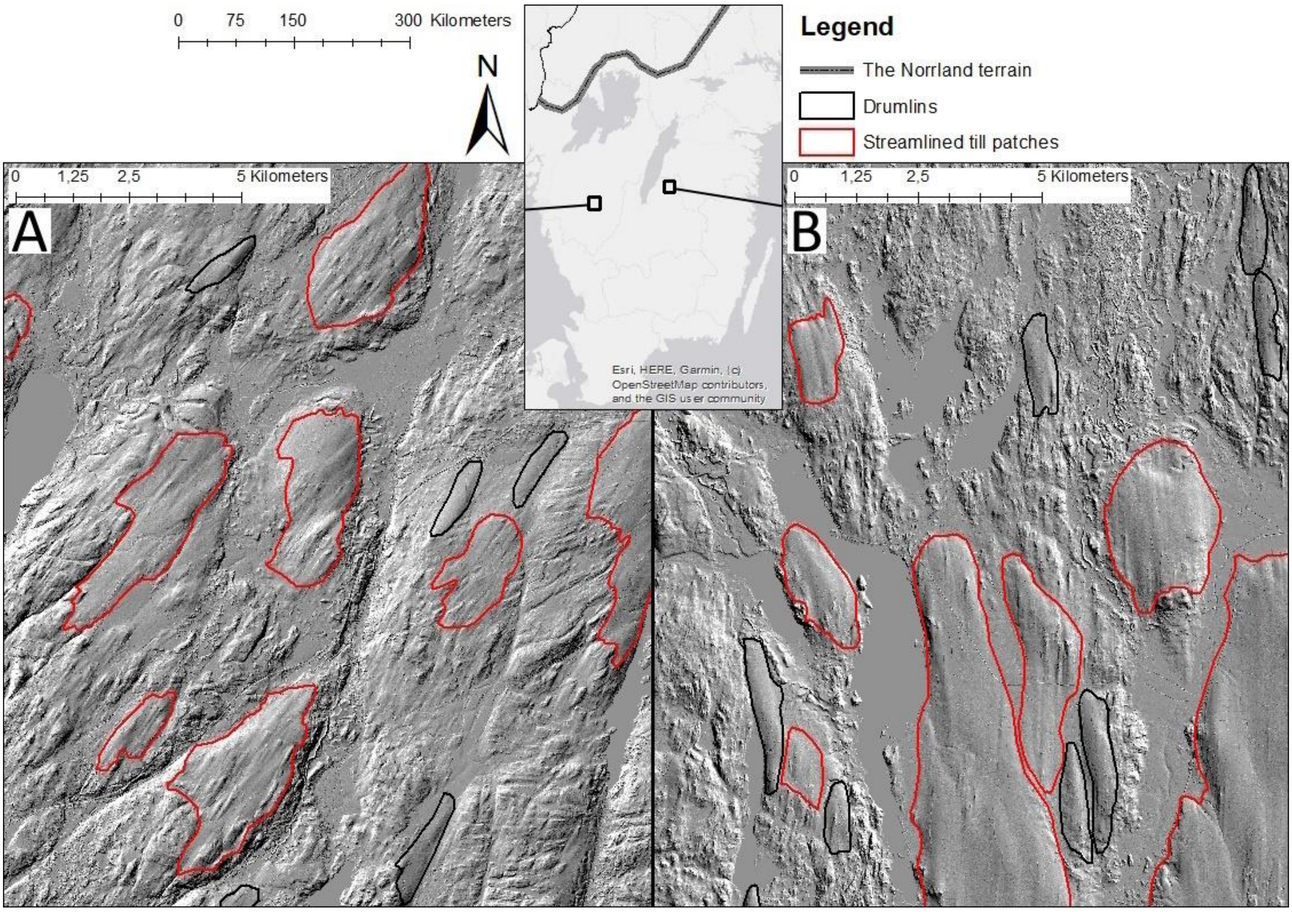

Figure 6. Detailed views of the drumlins and streamlined till patches. Location A is situated at the western side of the study area, whereas location B is located at the central part of the study area. The mapped drumlins and streamlined till patches are marked by outlined polygons, where drumlins have black outlines and streamlined till patches have red outlines. Data: © OpenStreetMap, contributors, CC-BY-SA and the GIS user community, © Lantmäteriet Elevation Data.

3.1.2 Regional distribution

Mapped drumlins and streamlined till patches, illustrated in figure 5, are shown to mainly be distributed in areas of an elevated and/ or eroded character (figure 3). This includes central Götaland and south-central Svealand. In contrast to these regions, the mapped landforms have rarely been observed at the flat surfaces of the sub-Cambrian peneplain. A distinct contrast is evident in eastern Småland, where relatively high relief topography meets the sub-Cambrian peneplain (figure 3).

The distribution of features for western and southern Götaland (figure 5) showcases instead, by comparing to eastern Götaland, a different pattern. Instead of the abrupt end of features, the mapped drumlins and streamlined till patches are instead gradually increasing in number from the coast and into the country. This trend is present in an eastern direction from western Götaland, and accordingly in a northern direction from the southern coast of Götaland. The relatively lightly distributed landforms found at western and southern coasts of Götaland are sited at the sub-Mesozoic hilly relief, whereas the bordering bedrock, sited at the South Swedish Upland, hold instead a higher distribution of features (figure 3). This bedrock is characterized by different erosional levels, shaping this undulating hilly relief

(Lidmar-Bergström, 2009). These erosional levels show higher vertical distance (height above sea level) as they extend further inland.

3.1.3 Geomorphometrics

Length, width, elongation ratio, area, spacing and height have been calculated for all features, as well for drumlins and streamline till patches separately. The morphometrics are shown in table 1.

Table 1. Measured morphometrical values from mapped drumlins and streamlined till patches. The values have been divided between all features, drumlins and streamlined till patches. The minimum, maximum and mean value are included, as well as the standard deviation.

All features (n=1187)	Minimum	Maximum	Mean	Standard Deviation
Length (m)	345.2	14443.0	2431.8	1530.1
Width (m)	99.9	5223.7	941.5	590.9
Elongation ratio	0.36	8.6	2.8	1.1
Area (km^2)	0.03	37.4	1.9	2.8
Spacing (m)	1.17	18749.8	1456.1	1883.1
Height (m)	3.8	79.8	30.7	13.6
Drumlins (n=379)	Minimum	Maximum	Mean	Standard Deviation
Length (m)	345.2	5911.9	2165.0	1032.3
Width (m)	99.9	1988.6	722.2	340.7
Elongation ratio	1.1	8.6	3.2	1.3
Area (km^2)	0.03	5.8	1.2	1.02
Spacing (m)	1.6	17060.4	2827.2	3005.9
Height (m)	6.0	75.7	29.7	13.3
Streamlined till patches (n=808)	Minimum	Maximum	Mean	Standard Deviation
Length (m)	437.2	14443.0	2557.0	1720.1
Width (m)	138.2	5223.7	1044.4	660.4
Elongation ratio	0.36	6.8	2.6	0.9
Area (km^2)	0.05	37.4	2.2	3.3
Spacing (m)	2.5	18749.8	1881.4	2358.3
Height (m)	3.8	79.8	31.1	13.7

3.1.3.1 Distribution of the morphometrics

The distribution of the morphometric parameters is illustrated in figure 7. The highest values for length, width, elongation ratio, area and spacing have been grouped respectively as they're sparsely distributed.

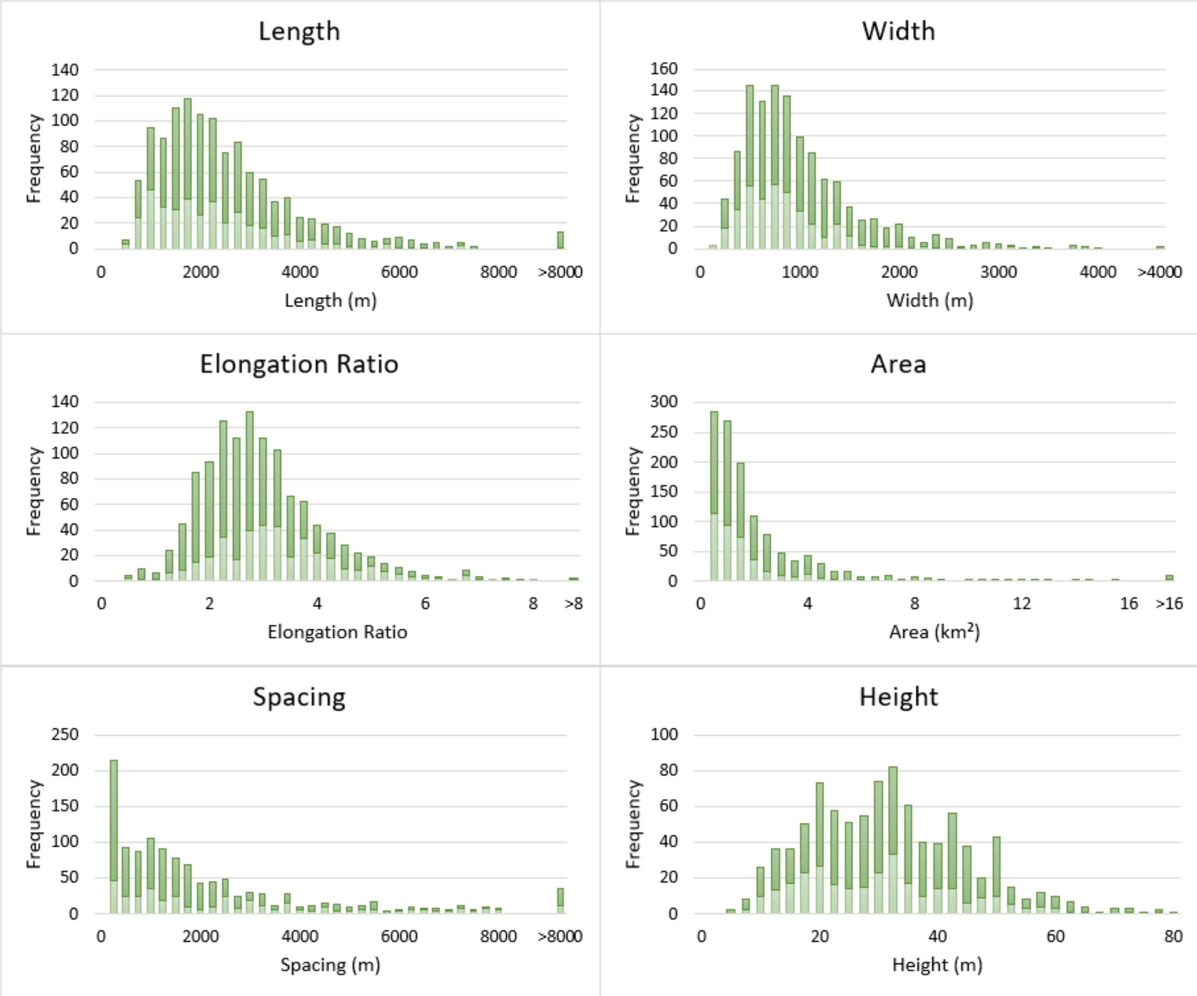

Figure 7. Distribution of the measured morphometrics for the mapped drumlins and streamlined till patches. The light green columns represent the drumlins, and the dark green columns represent the streamlined till patches.

3.1.3.2 Orientation of the mapped landforms

The orientation for each of the mapped features is illustrated in figure 8. Their direction varies across southern Sweden, with a predominant northeast trend in the west and a northwest trend in the eastern parts.

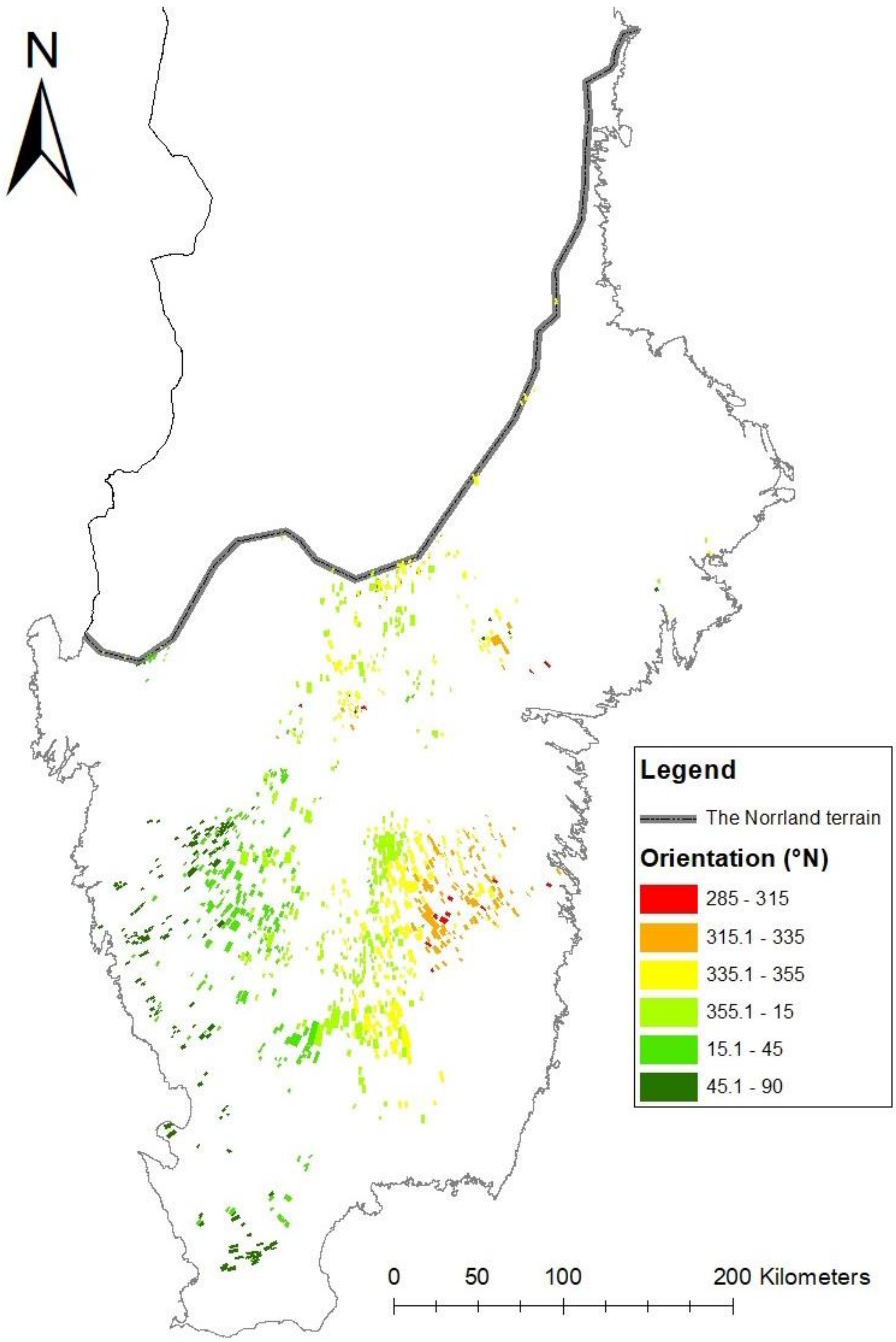

Figure 8. Distribution of mapped landforms, colored by their respective orientation. Data: © OpenStreetMap, contributors, CC-BY-SA and the GIS user community.

3.1.4 Statistical relationship between morphometrics

Correlation analysis has been conducted between length, width, elongation ratio, area spacing, and height (table 2). The correlation coefficients show generally weak relationships, with values typically close to 0. This is in contrast to perfect relationships, where values reach either 1 or -1. However, a few relationships stand out as considerably stronger, notably length vs width, length vs area and width vs area. All three relationships are well correlated for all features, as well for drumlins and streamlined till patches separately. Furthermore, length vs width, length vs elongation ratio, length vs area, width vs elongation ratio, and width vs area are the five only correlations that are statistically significant. This includes all features, as well as drumlins and streamlined till patches separately.

Table 2. The correlation between length, width, elongation ratio, area, spacing and height have been calculated using Pearson correlation coefficient. The values have been divided between all features, drumlins and streamlined till patches.

All features (n=1187)	Length (m)	Width (m)	Elongation ratio	Area (km²)	Spacing (m)	Height (m)
Length (m)	1					
Width (m)	0.72*	1				
Elongation ratio	0.27*	-0.33*	1			
Area (km²)	0.87*	0.80*	-0.0025	1		
Spacing (m)	-0.027	-0.013	-0.037	-0.035	1	
Height (m)	0.11	0.076	0.044	0.080	0.0036	1
Drumlins (n=379)	Length (m)	Width (m)	Elongation ratio	Area (km²)	Spacing (m)	Height (m)
Length (m)	1					
Width (m)	0.66*	1				
Elongation ratio	0.39*	-0.35*	1			
Area (km²)	0.85*	0.83*	0.061	1		
Spacing (m)	-0.049	-0.072	0.031	-0.058	1	
Height (m)	0.038	-0.039	0.077	-0.0025	0.032	1
Streamlined till patches (n=808)	Length (m)	Width (m)	Elongation ratio	Area (km²)	Spacing (m)	Height (m)
Length (m)	1					
Width (m)	0.72*	1				
Elongation ratio	0.26*	-0.32*	1			
Area (km²)	0.90*	0.79*	0.015	1		
Spacing (m)	-0.059	-0.067	0.037	-0.069	1	
Height (m)	0.088	0.11	-0.024	0.086	-0.023	1

* Statistically significant at α=0.05

The three strongest correlations from all the features, drumlins and streamlined till patches, length vs width, length vs area and width vs area (table 2), have been plotted against each other (figure 9).

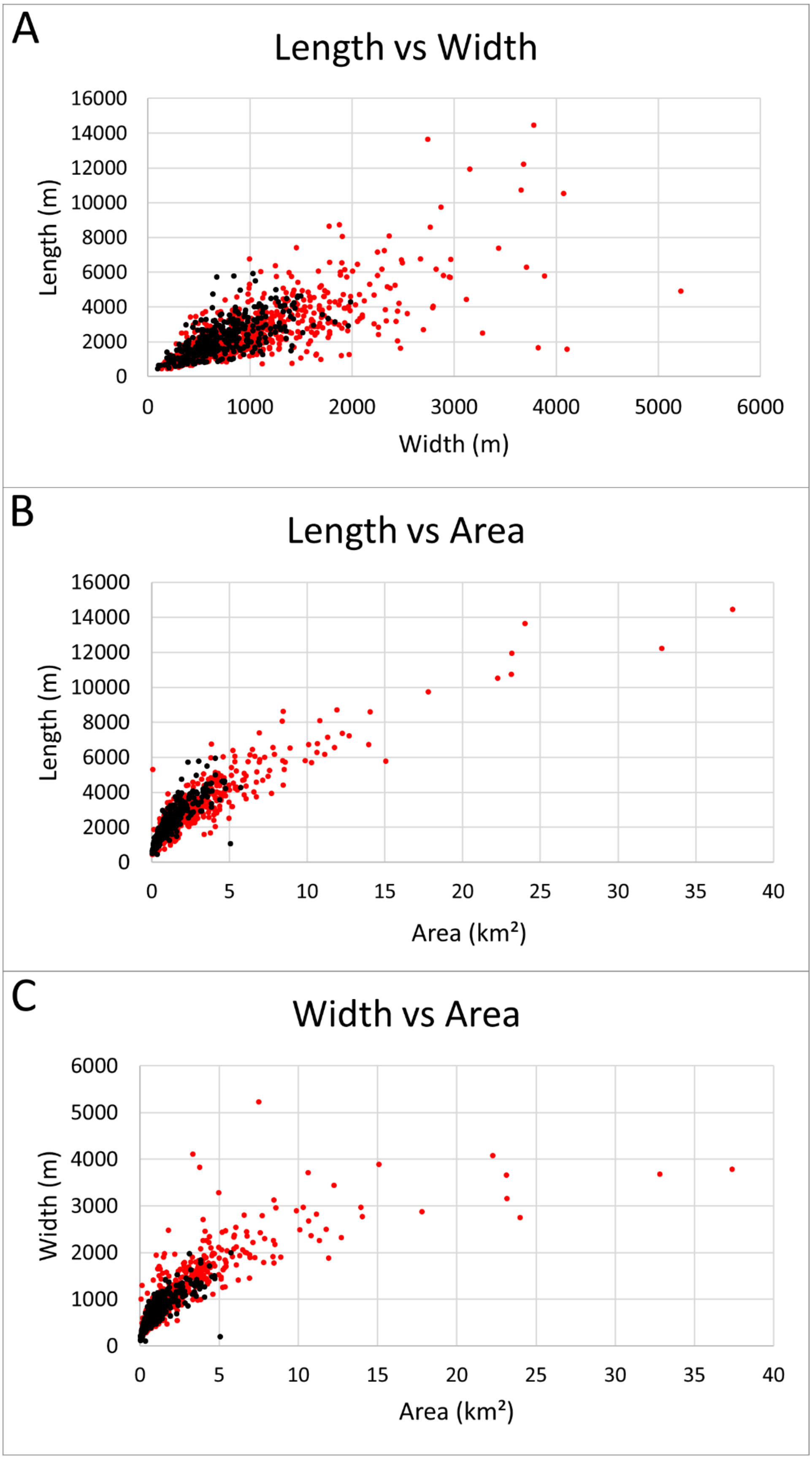

Figure 9. Length has been plotted against width and area (A and B) and width has been plotted against area (C). The black dots represent drumlins and the red dots represent streamlined till patches.

3.1.5 Presence of bedrock knobs in the features

Exposed bedrock knobs are present on 1083 out of the 1187 mapped features. The remaining 104 features are however uncertain as bedrock could be present within the landforms but is not exposed at the surface. Additionally, data from previous drillings and excavations has not provided a comprehensive interior view of any of the 104 features.

Bedrock knobs have been observed both within and at the margins of landforms, appearing on the stoss- and lee sides as well as in the central areas. 288 landforms have been observed with a majority of bedrock knobs at their lee side, 95 at the stoss side and 121 features with bedrock knobs at the central parts. The bedrock knobs for the remaining 579 are instead scattered over the landforms and can hence not be categorized into the three previous groups. Examples of bedrock knobs located mainly at the stoss- and lee side, in central and scattered over the landforms are illustrated in figure 10.

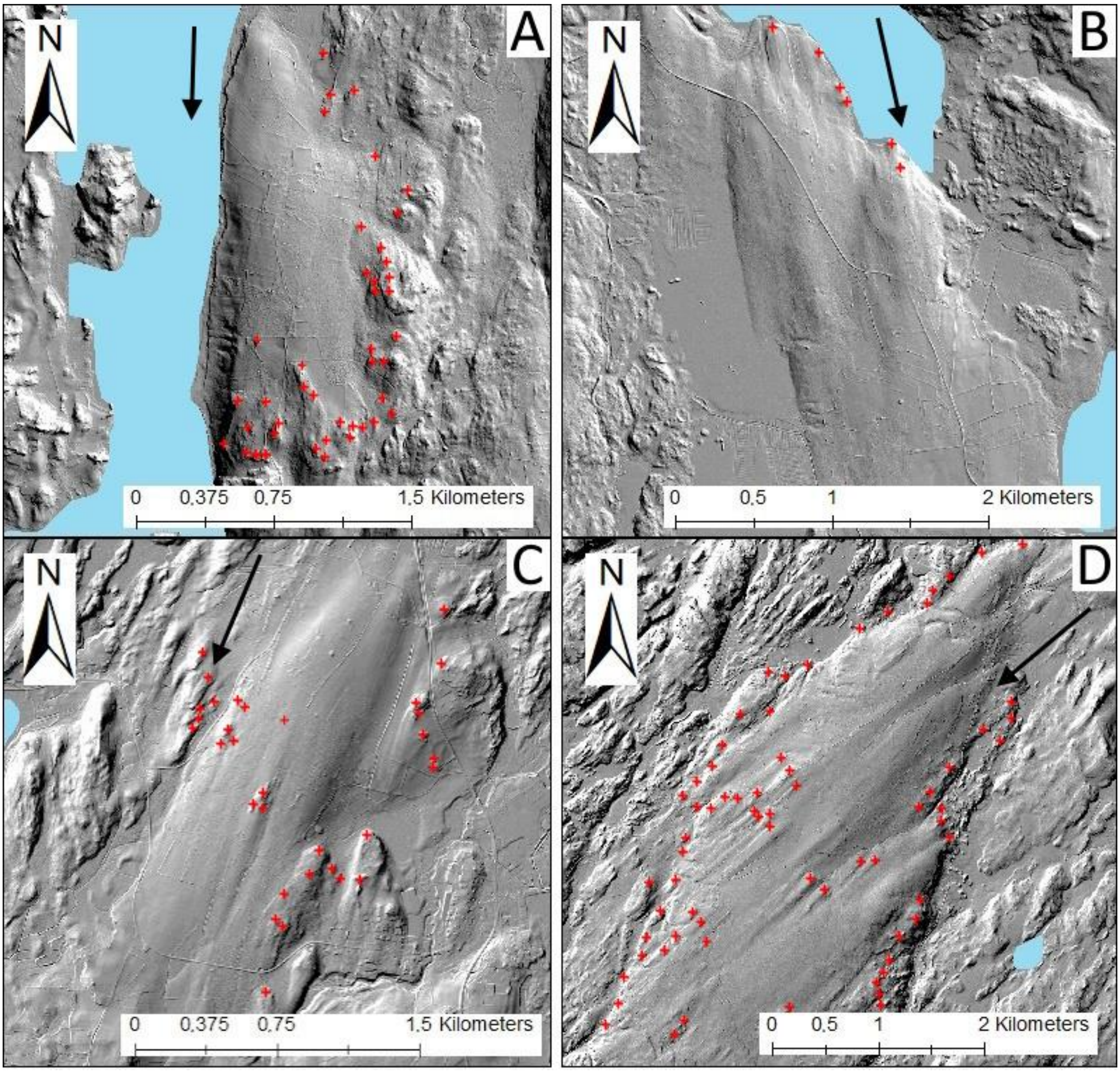

Figure 10. Examples of mapped features with influence of bedrock. (A) Landform with bedrock knobs on the lee side. (B) Landform with bedrock knobs on the stoss side. (C) Landform with bedrock knobs mainly in the central

parts. (D) Landform with bedrock knobs scattered all over. The black arrows show the direction of the ice. Red plus signs (+) marks bedrock knobs within and at the margins of the landforms. Data: © Lantmäteriet Elevation Data.

3.1.6 Previous drilling and excavation data

The SGU stratigraphic sequence database contains data from previous drilling and excavations for a total of 109 mapped landforms in the study area. In eight of these landforms have diamicton-covered sorted sediments been observed (table 3), while the remaining 101 contain diamicton exclusively. Among the 101 landforms were 78 drilled down to the bedrock, whereas the rest had an open ending. Additional data of table 3, concerning what type of observation that was conducted, the end, and coordinates are shown in appendix 5.

Table 3. Compiled data of previously drilled/ excavated sites from eight landforms, all streamlined till patches. The landforms have been named from A-H for increased clarity. Note that some landforms have had one site investigation, whereas others had multiple. These can be seen under the “Database-ID” column. As the original data were written in Swedish, “morän” has been translated to diamicton.

Landform	Database-ID	Depth from (m)	Depth to (m)	Observed material	Primary grain size	Secondary grain size	Genesis
A	BMW030072	0.0	3.0	Probed	Not classified	Not classified	Not classified
	BMW030072	3.0	8.0	Diamicton	Unspecified	Not classified	Till
	BMW030072	8.0	12.0	Diamicton	Clayey	Not classified	Till
	BMW030072	12.0	14.5	Sand	Fine sand	Not classified	Glaciofluvial sediment
B	ELM082032	0.0	25.0	Diamicton	Sandy- silty diamicton	Stony	Till
	ELM082032	25.0	30.0	Glaciofluvial sediment	Unspecified	Not classified	Glaciofluvial sediment
	ELM082032	30.0	33.0	Glaciofluvial sediment	Unspecified	Clayey	Glaciofluvial sediment
	ELM082032	33.0	35.5	Glaciofluvial sediment	Unspecified	Stony	Glaciofluvial sediment
C	EDA990064	0.0	2.0	Diamicton	Sandy diamicton	Not classified	Till
	EDA990064	2.0	2.2	Silt- sand	Coarse silt- fine sand	Not classified	Glaciofluvial sediment
	EDA990064	2.2	4.5	Diamicton	Sandy diamicton	Not classified	Till
D	SIS980170	0.0	1.5	Diamicton	Sandy diamikton	Not classified	Till
	SIS980170	1.5	1.8	Gravel	Gravel	Not classified	Glaciofluvial sediment
E	BMW188093	0.0	0.9	Organic material	Unspecified	Not classified	Organic material
	BMW188093	0.9	3.3	Diamicton	Sandy- clayey diamicton	Silty	Till
	BMW188093	3.3	4.3	Probed friction deposits	Fine clay	Not classified	Not classified
	CHO182001	0.0	0.5	Diamicton	Sandy diamicton	Not classified	Till
	CHO182001	0.5	2.5	Sand	Fine sand	Not classified	Glaciofluvial sediment
	CHO182001	2.5	4.0	Sand	Sand	Gravely	Glaciofluvial sediment
	CHO182001	4.0	5.0	Debris	Not classified	Not classified	Not classified
F	EDA901011	0.0	8.0	Unspecified	Unspecified	Not classified	Not classified
	EDA901011	8.0	15.0	Diamicton	Diamicton clay	Not classified	Till
	EDA901011	15.0	25.0	Sand- gravel	Sand	Gravel	Not classified
G	GRD082003	0.0	0.6	Diamicton	Sandy diamicton	Silty	Till
	GRD082003	0.6	3.0	Gravel	Gravel	Not classified	Glaciofluvial sediment
	GRD082006	0.0	0.4	Diamicton	Sandy diamicton	Not classified	Till
	GRD082006	0.4	2.0	Sand- gravel	Sand	Gravel	Glaciofluvial sediment
	JIG112102	0.0	1.5	Diamicton	Sandy diamicton	Not classified	Till
	JIG112102	1.5	8.6	Sand	Medium sand	Not classified	Glaciofluvial sediment
	JIG112102	8.6	9.5	Sand	Sand	Stony	Glaciofluvial sediment
	JIG112102	9.5	14.8	Sand	Medium sand	Not classified	Glaciofluvial sediment
	JIG112102	14.8	15.2	Diamicton	Diamicton, unspecified	Stony	Till
	JIG112103	0.0	1.5	Diamicton	Sandy diamicton	Stony	Till
	JIG112103	1.5	6.8	Sand	Sand	Not classified	Glaciofluvial sediment
H	EDA082018	0.0	1.0	Diamicton	Sandy diamicton	Not classified	Till
	EDA082018	1.0	4.0	Sand	Fine sand	Not classified	Glaciofluvial sediment
	EDA082019	0.0	1.5	Diamicton	Sandy diamicton	Not classified	Till
	EDA082019	1.5	2.5	Diamicton	Sand- silty diamicton	Not classified	Till
	EDA082019	2.5	4.0	Silt	Silt	Clayey	Glaciofluvial sediment
	EDA082020	0.0	2.0	Diamicton	Sandy diamicton	Not classified	Till
	EDA082020	2.0	2.5	Sand	Sand	Gravely	Glaciofluvial sediment
	EDA082020	2.5	3.5	Sand	Fine sand	Not classified	Glaciofluvial sediment

3.2 Field investigations

A total of eight samples were collected, around 1 kg respectively, at site 1.5, 3, 4.1, 4.2, 6.1, 6.3, 6.4 and 9. Sites located on the same landform were, for convenience, subdivided under the same main site number. Site 11 & 12 were however, despite being located on the same landform, divided into two to provide a clearer and more understandable overview of each respective site.

13 sites, comprising excavation/pit sites, cuts, and other depressions in the ground, have been visited and described across twelve different landforms. Each site is listed below.

3.2.1 Site 1

Five locations were investigated in and around a (presumably) old excavation site (figure 11, site 1). A few boulders were observed at the site and its surroundings. The first meter from the top of the western part of the excavation (sub-site 1.1) consisted of 90 cm fine-grained sand followed by 10 cm of medium sand. Approximately 1.5 m below the local top was about 70 cm of medium sand found horizontally into the wall. At the bottom of the pit, approximately 2 m down from the local top, was 50 cm of sorted gravel found. Due to the coarse material, no further investigation could be continued.
At the top of the central part of the excavation (sub-site 1.2), the first meter exclusively consisted of fine-grained sand. 1.3 m down from the local top was 1 m of medium sand revealed horizontally into the wall. Two additional investigations, 80 cm and 50 cm down from the local top respectively, uncovered 1 m of the same fine-grained sand found at sub-site 1.1. The bottom of sub-site 1.2, approximately 2 m down from the local top of the excavation pit exposed 20 cm of sorted gravel.
At the eastern part of the excavation pit (sub-site 1.3), the wall was examined horizontally 1 m down from the local top, and 60 cm of fine-grained sand was found. At the bottom of the pit, approximately 2 m down from the local top, 1 m of the same medium sand found in the walls of sub-site 1.1 and 1.2 was discovered.
An investigation conducted just south of the excavation pit (sub-site 1.4) revealed organic material.
Along the roadside east of the excavation pit (sub-site 1.5), presumably sandy diamicton was encountered. Due to uncertainties of the grain size, a sample (sample 1.6) was collected to bring back to the lab.

3.2.2 Site 2

Three different cuts were investigated along this landform (figure 11, site 2). However, after returning from the field, the exposures were judged to be meltwater channels. Only organic material was found at these three sub-sites, reaching between 50 cm-1 m down the surface. This material could possibly be peat. Boulders were observed at each site.

3.2.3 Site 3

At this location (figure 11, site 3), presumably an old excavation site, 50 cm of (silty-sandy) diamicton was identified horizontally into the wall of the excavation. 70 cm of the same material was found at the base of the excavation, about 5 m below the top of the site. A sample (sample 3) was collected at the base to investigate the grain size further. A few boulders were observed at this site.

3.2.4 Site 4

Two locations within the same cut were investigated, sited about 20 m apart (figure 11, site 4). This area is characterized by a significant amount of boulders. Horizontally into the cut (sub-site 4.1), diamicton was discovered almost immediately, to a depth of around 60 cm. The material appeared to be gravelly diamicton, but due to uncertainties, a sample (sample 4.1) was collected to bring back to the lab. Two diggings were made at this sub-site, approximately 1 m apart in elevation. The highest was located 50 cm down from the top of the cut. At sub-site 4.2, 60 cm of diamicton was encountered horizontally into the cut. However, this diamicton seems to contain finer material and less gravel compared to the diamicton found at sub-site 4.1. A sample (sample 4.2) was also taken here. Two investigations were made for this sub-site, approximately 1 m apart in elevation. The highest was located 50 cm down from the top of the cut.

3.2.5 Site 5

Two close-by exposures within the same site were investigated: 5.1 in a small cut and 5.2 at an old excavation/ pit (figure 11, site 5). Both sub-sites have a noticeable number of boulders present. Two locations within sub-site 5.1 were investigated, approximately 1 m apart in elevation. Around 45 cm of sandy diamicton were revealed horizontally into the wall at both locations. The highest was located 50 cm down from the top of the cut. The same sandy diamicton was identified at the wall of the old excavation (site 5.2), as well as down at its base. The sampling reached to a depth of 50 cm for both the vertical and horizontal investigation, as the boulders and stones present made it hard to go deeper. The investigation of the wall was made twice, 1 m apart in elevation. The highest was located 1 m down from the top of the wall.

3.2.6 Site 6

This site is located at a presumably old excavation site (figure 12, site 6). The area is somewhat boulder-strewn. Approximately 4.5 m down from the local top of the excavation site (sub-site 6.1), the wall was dug horizontally. The first 15 cm consisted of sandy diamicton, followed by 80 cm that appears to be very sandy diamicton. Due to this uncertainty, a sample (sample 6.1) was collected for the lab. Sub-site 6.2 is situated approximately 2 m above (in elevation) sub-site 6.1 and 3 m down from the local top of the excavation site. Similar layers as for sub-site 6.1 was discovered horizontally into the wall, where the first layer consisted of 15 cm of sandy diamicton, followed by 50 cm of the same very sandy diamicton found previously. At the bottom of the excavation site (sub-site 6.3), 1 m of sand was found vertically down in the ground. It’s judged that the sorted sediment prior to the old excavation was located below the former surface of the landform, and a layer of diamicton. A sample (sample 6.3) was taken here. A big root wad was discovered near the top of the excavation site (sub-site 6.4), with its base approximately 90 cm down from the local top. Sandy diamicton was identified here. A sample (sample 6.4) was taken 15 cm under the base of the root wad.

3.2.7 Site 7

This site is located within a cut in the terrain (figure 12, site 7). About 30 cm of sandy diamicton was found horizontally into the wall of the cut, approximately 2 m below the top. The investigation at the base (approximately 3.5 m below the top of the cut) revealed a similar pattern with the same sandy diamicton extending about 50 cm down from the surface. The first meter at the top of the cut contained around 75 cm of sandy diamicton. Numerous boulders are scattered all over the site.

3.2.8 Site 8

This location raises suspicions of anthropogenic influence as it's sited in an urban environment (figure 12, site 8). The first horizontal investigation of the cut, about 1 m in elevation above the road, unveiled about 50 cm of sandy diamicton. A subsequent investigation, 1.5 m in elevation above the initial point (1.5 m below the top of the cut), revealed the same sandy diamicton as found below. The first meter at the top of the cut revealed about 60 cm of sandy diamicton. No visible boulders were noted.

3.2.9 Site 9

This site is located in a depression, approximately 1 m down from the surrounding terrain (figure 12, site 9). At its base, organic material was encountered from the surface and 30 cm down, until no deeper investigation was possible due to the presence of boulders. The first meter was investigated at the top of the depression, where about 70 cm of (sandy-silty) diamicton was found. A sample (sample 9) was collected here to investigate the grain size further in the lab.

3.2.10 Site 10

Located on sloped terrain (figure 12, site 10), sub-site 10.1 and 10.2 are both positioned approximately 3.5 m down from the top of the slope. 30 cm of organic material were found at each site, which included both vertical and horizontal investigations. A few boulders were found at this location.

3.2.11 Site 11

Sited within a depression in the terrain (figure 13, site 11), many boulders were observed at this site. The base of the depression lies approximately 1 m down from the surrounding terrain. The first meter was investigated from top of the depression, where about 70-80 cm of sandy diamicton was found. From the base of the site, about 50 cm of sandy diamicton was identified downwards.

3.2.12 Site 12

Two locations within the same cut were examined (figure 13, site 12); one at the wall of the cut (sub-site 12.1) and the other at the base (sub-site 12.2). Numerous boulders are located within this site. At sub-site 12.1, approximately 2 m down from the top of the cut, 1 m of organic material was observed horizontally. Attempts to dig further into the wall were hindered by the abundance of boulders. The lowest accessible point within the cut (sub-site 12.2; approximately 50 cm further down from sub-site 12.2) was investigated vertically down in the ground. About 30 cm of sandy diamicton was found. Further investigations were impeded by the amount of boulders present.

3.2.13 Site 13

Five locations were investigated along a great sloped area (figure 13, site 13). Here, fairly many boulders could be observed. About 12 m down from the top of the slope (sub-site 13.1), 50 cm of sandy diamicton was revealed horizontally into the wall. Approximately 10 m down from the top of the slope (sub-site 13.2), 1 m of organic material was found horizontally into the slope. 1 m of organic material was also found horizontally into the slope approximately 3.5 m down from the slope top (sub-site 13.3). Lastly, at the top of the slope (sub-site 13.4), about 90 cm of material was investigated downwards, to reveal organic material.

3.2.14 Detailed view of field investigation

A detailed view of each visited site, including the sub-sites, are presented in figures 11, 12 and 13. Site 1-5 are illustrated in figure 11, site 6-10 in figure 12 and site 11-13 in figure 13.

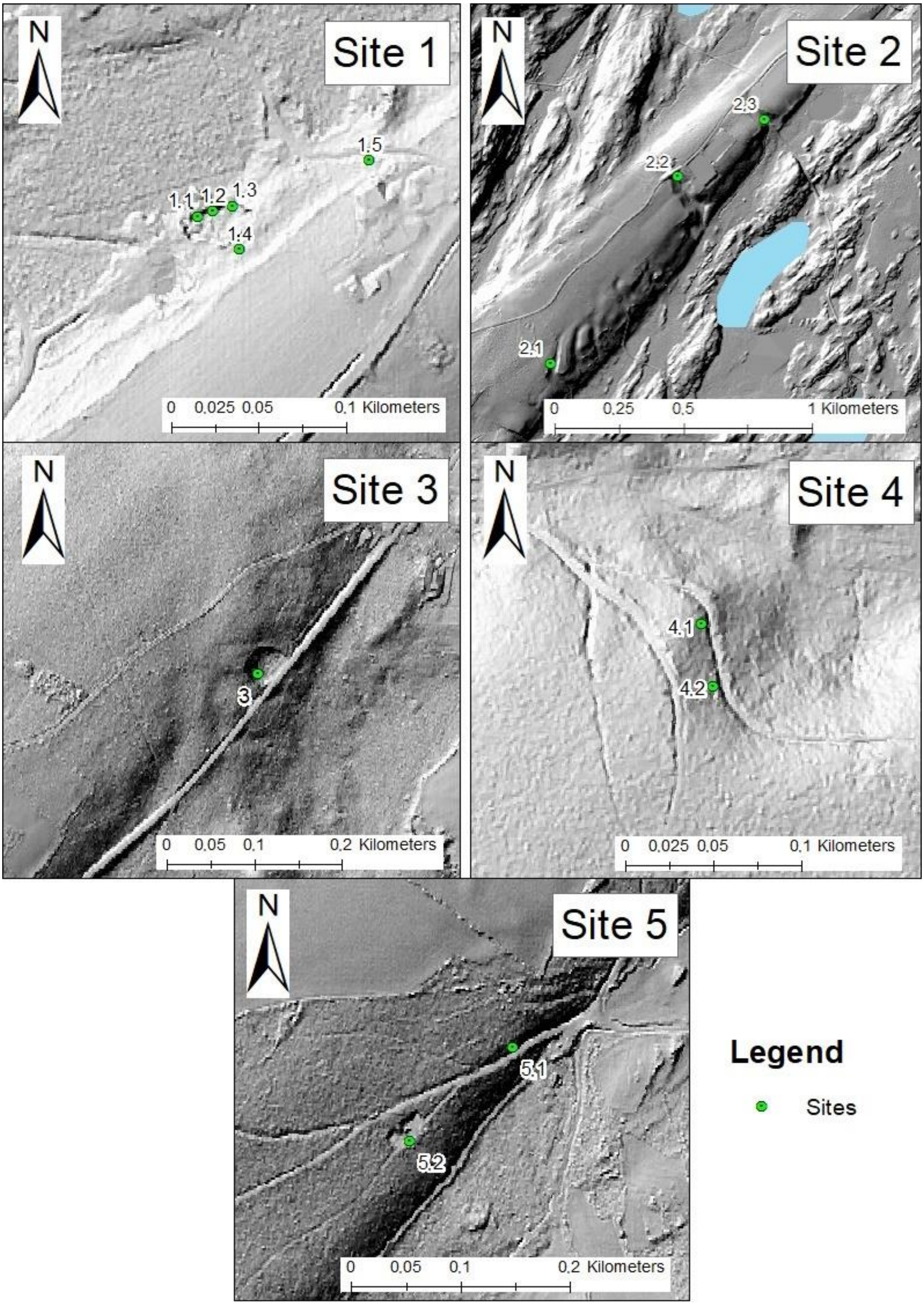

Figure 11. Detailed views of the location of each site, illustrating site 1-5. Data: © Lantmäteriet Elevation Data.

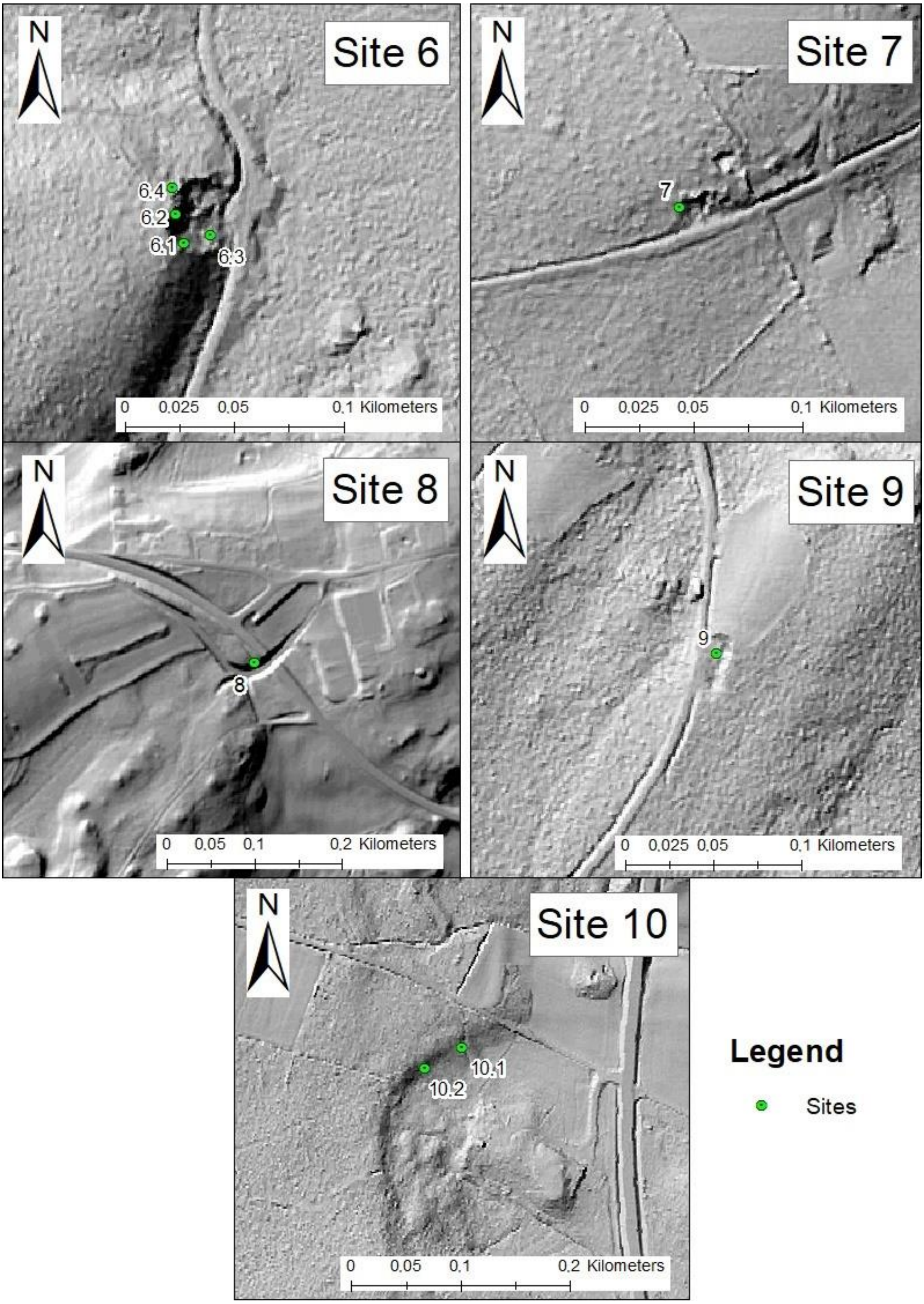

Figure 12. Detailed views of the location of each site, illustrating site 6-10. Data: © Lantmäteriet Elevation Data.

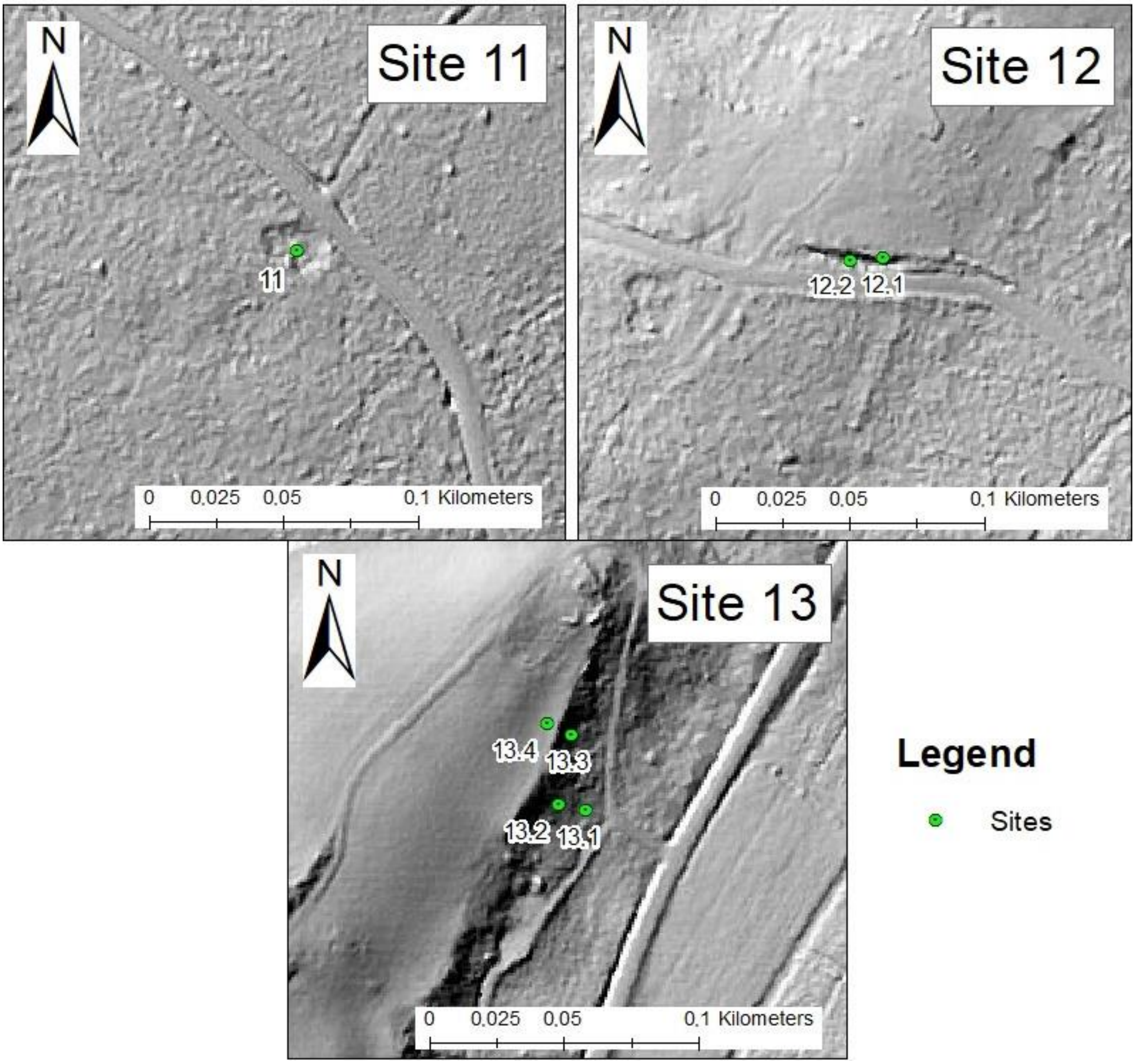

Figure 13. Detailed views of the location of each site, illustrating site 11-13. Data: © Lantmäteriet Elevation Data.

3.3 Grain-size analysis

The grain-size distribution from the sieve- and hydrometer analysis have been divided between the fractions of gravel, sand, silt, and clay, and are illustrated for each sample. The distribution has also been illustrated through diagrams. Table and diagrams are based on data located in appendixes 6.A-H.

3.3.1 Grain size distribution between fractions

The distribution of grain sizes, divided between gravel-, sand-, silt- and clay fractions are shown for each sample in table 4. Note that the silt- and clay fractions are not adding up to the fine material. For the silt, only the largest and smallest grain sizes measured through hydrometer analysis within the silt fraction are included. An approximate value is therefore shown. For the clay, the nearest measured grain size to the clay grain size limit (0.002 mm) is included, which also has resulted in an approximate value.

Table 4. Percent mass of gravel, sand, and fine materials (silt and clay) determined for each sample.

Sample	Gravel (%)* (63 mm-2 mm)	Sand (%)* (2 mm-0.063 mm)	Fine material (%)* (<0.063 mm)	Silt (%)** (0.063 mm-0.002 mm)	Clay (%)** (<0.002 mm)	Determined material
1.6	28.4	54.2	17.2	10.4	3.5	Sandy-gravely diamiction
3	19.4	54.7	25.6	16.9	4.1	Sandy diamiction
4.1	25.6	52.0	22.1	13.2	5.6	Sandy-gravely diamiction
4.2	18.1	52.0	29.4	18.9	4.5	Sandy diamicton
6.1	22.2	59.8	17.5	10.6	4.2	Sandy-gravely diamiction
6.3	1.0	73.4	25.2	14.9	5.9	Sand
6.4	15.7	53.9	30.1	20.2	4.2	Sandy-silty diamicton
9	14.8	54.2	30.7	25.2	5.2	Sandy-silty diamicton

* Determined by sieve analysis.
** Determined by hydrometer.

3.3.2 Cumulative grain-size distribution

The cumulative weight obtained from the sieve- and hydrometer analysis have been combined for each sample and are illustrated in figure 14. These are based on the same data as table 4.

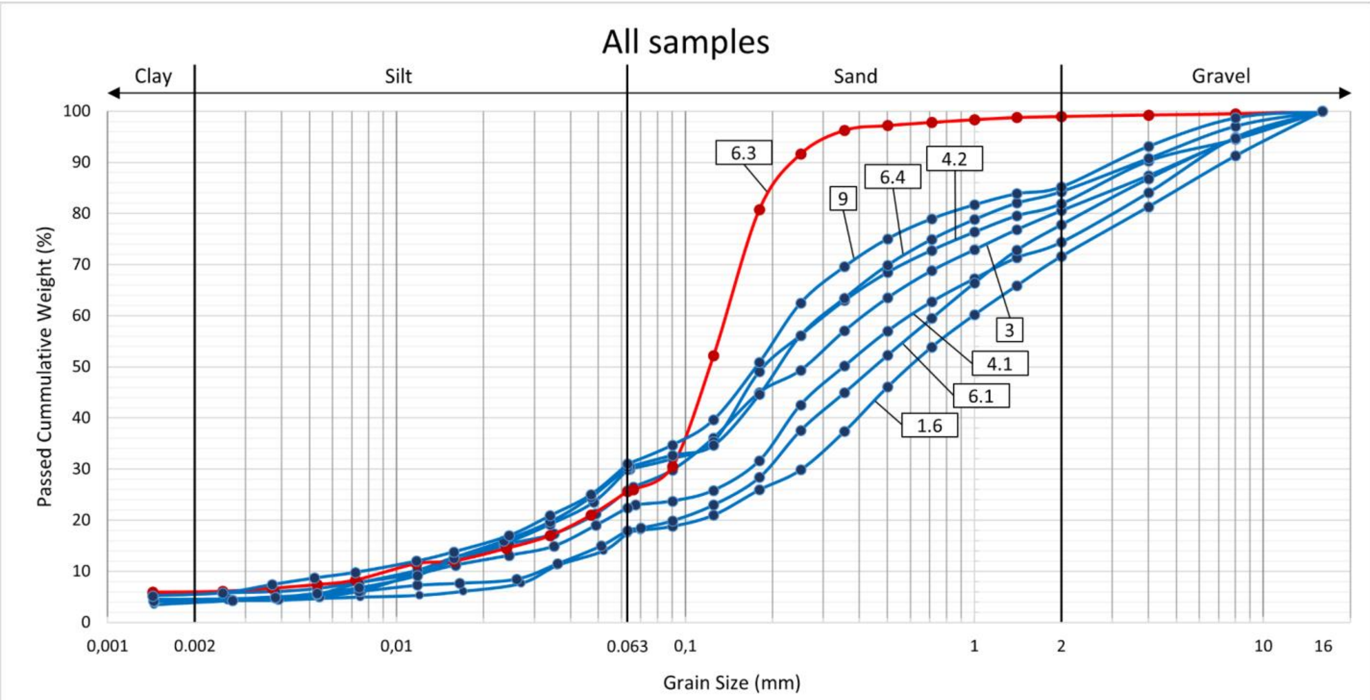

Figure 14. The cumulative grain size distribution for all samples, with results from the sieve- and hydrometer analysis combined. The blue lines are samples determined to be diamicton, and the red line is determined to be sand. The diagrams are based on data from appendixes 6.A-H.

4 Discussion

4.1 Morphometric comparison with other streamlined landforms

The mapped drumlins and streamlined-till patches typically exhibit a larger size than other streamlined bedforms found in Sweden and elsewhere (Clark et al., 2009; Dowling et al., 2015; Möller & Dowling, 2016; Sookhan et al., 2022). This has in particular been observed for the length, width and height. Drumlins mapped in this study are generally smaller than the mapped streamlined till patches (table 1), but still larger than drumlins mapped in other studies. The study by Dowling et al. (2015) shows over 10 000 mapped drumlins, have measured the mean value of length to 461 m, the mean value of width to 104.6 m and the mean value of height to 4.8 m. This is to compare with the morphometric of the drumlins in this study, where the landforms are (in mean) over 4.5 times longer, almost seven times wider and over six times higher. The authors however highlight that the mapped features are generally smaller than streamlined bedforms found elsewhere.
Length, width, and height of the mapped drumlins are furthermore greater than drumlins identified on the Närke plain in south-central Sweden (Möller & Dowling, 2016). The elongation ratio of the drumlins in this study is however (in mean) smaller compared to the drumlins identified by Möller and Dowling (2016). The study by Clark et al. (2009) has moreover compiled fifty investigations of drumlins (between 1906-2007) from mainly Europe, but also Canada and the USA, where the mean value for length is 634 m, 241 m for width and 3.4 for the elongation ratio. Length and width are distinctly smaller than features mapped in this study, whereas the elongation ratio, with a ratio of 3.2 in this study, is closer. The high standard deviation values for the length and width should however be noted as they show great variations of values from the respective mean (table 1 and figure 7).

On other hand, Vikberg-Samuelsson et al. (2022) has measured similar morphometry of Lid moraines (overlaps in many ways with drumlins and streamlined till patches) compared to this study, specifying length between 1-4 km, approximately 1 km in width and between 10-30 m in height. Moreover, the orientation measured for the drumlins and streamlined till patches largely coincide with the regional direction of the last ice (ibid, following the interpretation by Perhans, 2002).

4.1.1 Correlation comparison of morphometrics

The correlations between length vs width for all features as well for drumlins and streamlined till patches separately (table 2) stands out as some of the stronger relationships in this study. Clark et al. (2009) and Johnson et al. (2010) also found the same relationship for drumlins, although with a coefficient value of 0.45 and 0.46 respectively, indicating a weaker correlation compared to the findings of this study.

The strong correlations between area vs length and area vs width (table 2) respectively were expected, as both length and width generally increase when the area of the landform increases.

In this study, the correlation (for drumlins) between height and other morphometric parameters are found with very weak relationships, as well as not being statistically significant (table 2). However, previous studies have found statistically significant correlations between height and other parameters for drumlins. For example, Spagnolo et al. (2012) and Dowling et al. (2015) have both determined correlations between height vs length, width, and area, with Spagnolo et al. (2012) also concluding a relationship between height and elongation ratio. While these four relationships are not particularly strong, they're still stronger than the same relationships found in this study.

4.2 Internal structure of drumlins and streamlined till patches

Among the 13 visited sites, diamicton was found at all except one (site 2); greater amount of organic material was found at site 2; diamicton-capped sorted sediment was found in site 6, and sorted sediment (without an overlying layer of diamicton) was found at site 1. The last one is however not considered to have been deposited proglacial, as SGU has marked the material of postglacial origin (observed through *the Quaternary map viewers* offered by SGU, 2024b). The same interpretation was made in this study using LiDAR. The compiled previous drilling and excavation data (table 3) revealed a similar pattern, where most landforms contained only diamicton and a smaller number were observed with sub-till sediment.

4.2.1 Sub-till sediment

4.2.1.1 Presence of landforms with sub-till sediment

A smaller number of drumlins and streamlined till patches has been identified with sorted sediment below the surface diamicton in this study: one from the field investigation (site 6.3) and eight from compilation of previous drillings and excavations. However, previous studies have observed sub-till sorted sediment beneath streamlined formations in southern Sweden. Möller and Murray (2015) and Möller et al. (2020) have for example identified and analyzed several landforms with sub-till sediment in south-central Sweden, in Småland. Möller and Murray (2015) analyzed the features through dug trenches, whereas drillings were conducted by Möller et al. (2020). Data from six of these features were not found in the SGU database, adding additional landforms observed with sub-till sediment to the study area. Five of them were found in Möller and Murray (2015) and one from Möller et al. (2020). The latter study did however make additional investigations in two of the landforms first investigated by Möller and Murray (2015), where they drilled. Their respective core logs are illustrated in appendixes 7.A-C, three from drilling and three from dug trenches. North of these findings, Bergström et al. (2019) documented prominent landforms characterized by sorted sediment covered with diamicton. These are located east of Vättern, close to Tranås. Ising (2012) has also found similar landforms around Tranås, although he suggests that the presence of sorted sediment within these landforms is only a possibility. These two studies have however not been as carefully analyzed as the studies conducted by Möller and Murray (2015) and Möller et al. (2020), where neither the quantity of features nor the specific type or genesis of sorted sediment are specified.

4.2.1.2 Origin of sub-till sediment

Möller and Murray (2015) suggests that sorted sediment from a previous glaciation could have been deposited, and later partly eroded and shaped, to later become covered by till. Based on Optically Stimulated Luminescence (OSL)-dating of the sorted sediments, the authors suggests that the material was deposited before the last glaciation, during Marine Isotope Stage 3 (MIS 3), between approximately 60 000–30 000 years ago (Möller & Murray, 2015). The age interval is well correlated with the suggested time span for the Ristinge and Klintholm ice advances into Denmark, as the respective advance moved in from the east over southern Sweden and through the Baltic Basin into Denmark (Houmark-Nielsen, 2004, 2010, 2011; Larsen et al., 2009a, 2009b). The top layer of diamicton has furthermore been interpreted by Möller and Murray (2015) and Möller et al. (2020) to originate from the last glaciation, as the advancing ice sheet picked up and transported loose material and parts of the bedrock to later deposit it (SGU, 2020b).

An area with traces from one glaciation would (simply explained) have a depositional sequence (if complete) of diamicton at the bottom, overlayed by sorted sediment. An area with traces of two glaciations would however, if complete sequences, include diamicton at the bottom (from an earlier glaciation), overlayed by sorted sediment, followed by another layer of diamicton (from a later glaciation) and lastly sorted sediment at the top. Despite that landforms and deposits normally are eroded and redeposited by the succeeding glaciation, these can sometimes be preserved due to their position in the terrain or characteristics of the last glaciation (Vikberg-Samuelsson et al., 2022). For example, studies investigating old sediments and landforms in northern Sweden suggests that a cold-based ice could have preserved the underlying material and landforms (e.g. Kleman,1994; Kleman & Glasser, 2007; Kleman & Stroeven, 1997; Lagerbäck, 1988). The movement of the cold-based ice sheet was due to deformation of the ice mass, rather than basal sliding, as indicated by Blomdin et al. (2021). Materials and landforms from a previous glaciation and ice-free periods can hence be preserved from being eroded away.

4.2.1.3 Interpretation of the sub-till sediment found in this study

Although no dating of the sediment was taken in this study, the sorted sediment may be considered older relative to the overlaying surface till, as the material might be related to meltwater deposition during a previous glaciation. This has also been interpreted by previous studies (e.g. Alexandersson, 2010; Lagerbäck, 2018; Möller, 2010; Möller & Murray, 2015; Möller et al., 2020; Vikberg-Samuelsson et al., 2022).
Previous drilling and excavation data compiled from the SGU database shows two “almost complete” sequences, with glaciofluvial sediment in between two layers of diamicton (landforms C and G in table 3). It's interpreted that these two originate from deposits from two glaciations, where a top layer of glaciofluvial material could have been eroded away, if deposited at all. The lower diamicton is assumed to originate from an earlier glaciation relative to the upper diamicton, which in turn likely was deposited during the last glaciation. The glaciofluvial sediment are interpreted to have been deposited during an intervening deglaciation period, and consequently partly eroded and shaped by the last glaciation before overlain by a cover of till, as suggested by Möller and Murray (2015). The presence of coarser sediment suggests that a higher meltwater flow occurred from a retreating ice sheet, where the material was transported and deposited in front of the ice (as suggested by Karlsson et al., 2021). Conversely, the finer material present would instead have been

transported further away from the margin and to settle in quiet waters (as suggested by Karlsson et al., 2021). It’s interpreted that silt and clay may have been deposited in the still waters of glacial lakes formed between the ice margin and topographic higher terrain as the ice melted (as suggested by Lundqvist, 2009). Similar interpretations have also been made by Möller et al. (2020) and Vikberg-Samuelsson et al. (2022).
The remaining drill holes and excavations in table 3 reveal a layer of diamicton overlying glaciofluvial sediment. These formations are also suggested as evidence of two separate glaciations, and thus followed the same processes as the two landforms above (but without deposit of the bottom layer of diamicton).

It's hence interpreted that erosion stands as the primary driving force behind the formation of till-capped sorted sediment. Depositional processes would however too have been active due to the emplacement of till. This has also been suggested by Möller and Murray (2015). This theory is hence a likely explanation for the origin of sub-till sediment identified in this study.

4.3 Regional trends

4.3.1 Distributional comparison between drumlins and streamlined till patches

Comparing the distribution between drumlins and streamlined till patches identified in this study (figure 3), no apparent difference can be distinguished. The distribution between the two landforms also seem to mainly coincide when comparing streamlined till patches with a wider dataset of drumlins, with over 10 000 drumlins mapped by Dowling et al. (2015). The distribution of drumlins in Dowling et al. (2015) seems to, like in this study, be located in areas with an abundance of elevated bedrock terrain. However, a notable distributional difference is seen in the southern parts of Småland, where the drumlins by Dowling et al. (2015) are much more present. This contrast could suggest that the relatively smaller relief that characterize this area (figure 3) may contribute to smaller landforms. This has also been suggested by Påsse (1988).

4.3.2 Subglacial meltwater corridors

Mapped drumlins and streamlined till patches in this study have been observed bordering on hummock corridors, as mapped in southern Sweden by Peterson-Becher and Johnson (2018), Peterson-Becher et al. (2017) and Öhrling et al. (2020). Hummock corridors are believed to be evidence of former extensive subglacial meltwater flow under the ice sheet (Lewington et al., 2019). This suggests that drumlins and streamlined till patches with edges similar to the margins of hummock corridors have been eroded and isolated from each other. In similarity to this, hummock corridors both incised (figure 15A) and partly incised (figure 15B and 15C) into drumlinised surfaces have been highlighted by Petersson-Becher and Johnson (2018).

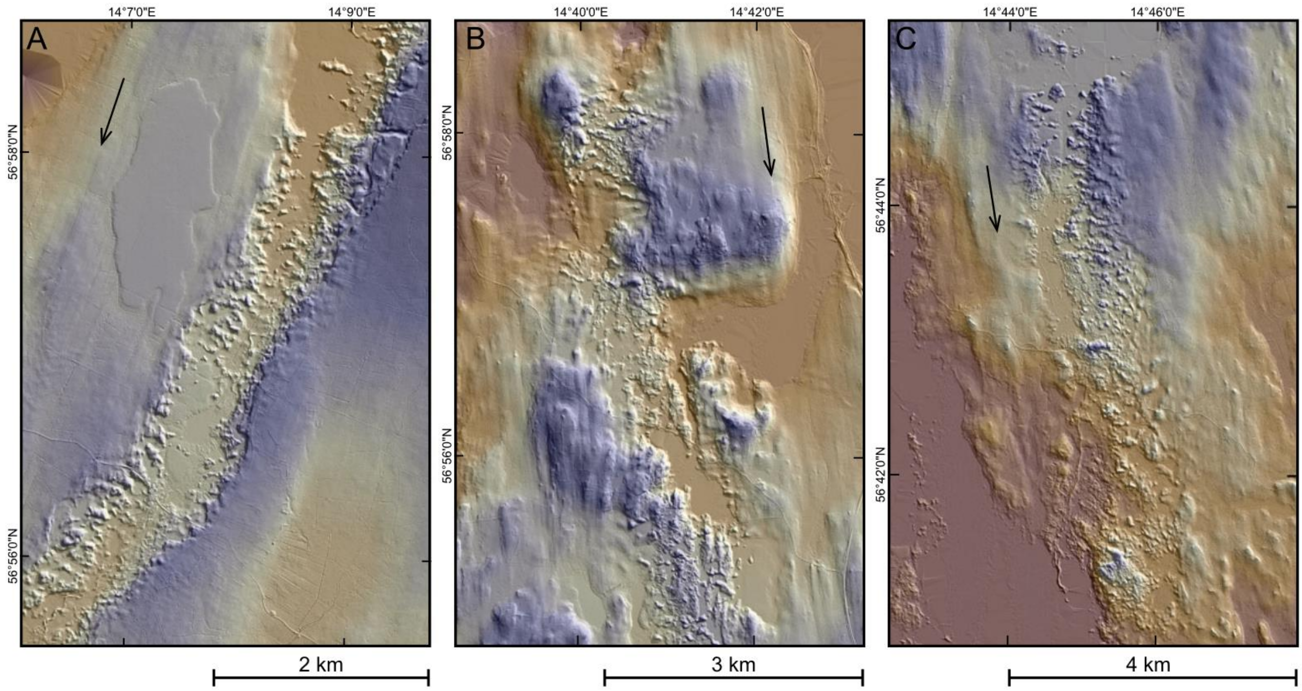

Figure 15. Examples of hummock corridors. (A) Hummock corridor incised in a drumlinised till surface. (B and C) Hummock corridor that is partly incised/ partly with positive (upstanding) form. Both are surrounded by drumlinised till. The black arrows are showing the direction of the local ice-flow. From Petersson-Becher and Johnson (2018).

4.4 Impact of physiographic features

Drumlins and streamlined till patches are mainly sited on undulating hilly relief surfaces, and bedrock knobs are a predominant feature identified at the surfaces and margins of the identified drumlins and streamlined till patches. The distribution of landforms is additionally seen to have been formed in connection to residual hills (mainly in central Småland), as well as around fault-line scarps (figure 3; in mainly Scania and south-central Svealand). A residual hill formed when surrounding bedrock has eroded away, leaving the hill standing higher than the terrain around. This typically occurs in regions where differential erosion has taken place, leaving behind more resistant rock formations as hills or ridges while softer materials erode away (Lidmar-Bergström, 2009).
It is hence interpreted that prominent elevated areas may control the location of the identified drumlins and streamlined till patches, where material was able to accumulate at these topographic heights or that sediment was removed from lower areas in between. Hart (1997) suggests that rock-cored drumlins may have been formed by deformation and plastering on of sediment around an elevated bedrock, combined with accumulation of material into a downstream cavity formed in the ice by pressure from the bedrock. As a part of this process, material is also likely to have been captured around bedrock knobs or rock escarpments, as suggested by Boulton (1987).

Due to the identified drumlins and streamlined till patches distinguishable size in the landscape (as discussed earlier), it's believed that the presence of large, elevated areas (large relative to southern Sweden) could favor accumulation of a greater amount of material (compared with smaller drumlins seen in for example Clark et al., 2009 and Dowling et al., 2015).

The distribution of drumlins and streamlined till patches in this study is evidently controlled by the characteristics of the bedrock. However, it remains unclear why the physiographic features influenced an uneven distribution of the mapped landforms from Eastern and Southern Götaland to central Småland, as a greater number of drumlins and streamlined till patches are found within the South Swedish Upland compared to the sub-Mesozoic hilly relief, despite being of an undulating character. This suggests that aspects beyond physiography may be at play that have affected the distribution patterns.

4.5 Genesis of drumlins and streamlined till patches

Numerous studies (e.g. Hart, 1997; Menzies, 1979; Stokes et al., 2012) suggest that drumlins can be categorized based on three main processes influencing their formation: erosional, depositional, and deformational. Hart (1997) argues that landforms can arise from a single process, a combination of two processes, or an intermix of all three. In the study area, the presence of drumlins and streamlined till patches, along with their specific distribution as shown in figure 5, are attributed to these processes. Erosion and deposition are considered in this study. This study has however not addressed evidence of deformation as suitable exposures for such investigation was not analyzed.

4.5.1 Evidence for erosion

The presence of older sub-till sediment in relation to the overlying layer of till suggests that erosion has played a significant role in shaping the drumlins and streamlined till patches. Additionally, as hummock corridors are bordering mapped features, it's interpreted that the margins of drumlins and streamlined till patches may exhibit modifications by meltwater erosion, further supporting the erosive processes at play.

The existence of bedrock knobs could moreover have acted as a protective barrier, sheltering sediment from being eroded away. This could hence have given rise to not only crag and tails, but drumlins sited at the stoss side of the knobs. The presence of bedrock knobs could furthermore suggest protection from erosion of broader areas, where some drumlins and streamlined till patches remained preserved as the bedrock knobs didn’t allow deep erosion. The erosional processes are illustrated in figure 16A, where sorted sediment and till have only been partially eroded, being protected by bedrock.

4.5.2 Evidence for deposition

The till composing the drumlins and streamlined till patches serves as clear evidence of deposition, with the material likely originating from the most recent glaciation. Although the deposition of till later was eroded into the form the landforms have today (figure 16A), deposition played a significant role in the formation of these landforms. As mentioned in 4.5.1, the presence of bedrock knobs could have acted as protection from the erosion. Depositional processes are illustrated in figure 16B, showcasing till deposition and accumulation on undulated hilly terrain.

In the study by Remmert et al. (2022), stratigraphic evidence for subglacial deposition into the drumlin form at Dösebacka was revealed. The primary forming process was by accretion (successively accumulation of sediment) (Remmert et al., 2022). Erosion has also been interpreted to have occurred as older sediment was found at the lowest parts of the drumlin (ibid). The Dösebacka drumlin is located within the study area.

The presence of sorted sediment observed within some of the mapped landforms could have induced the deposition of till, resulting in emplacement of till over the sorted sediment (as exemplified in figure 16C). Sandy sediment covered by till has been found in many landforms in Sweden, both in this study (one from the field investigation (site 6.3) and six from the compilation of previous drillings and excavations (landforms A, C, E, F, G and H in table 3)) as well as in previous research (e.g. Möller & Murray, 2015; Möller et al., 2020). The deposition of till may have occurred because the ice traveled over permeable sand, where the loss of water into the sand allowed till to be deposited.

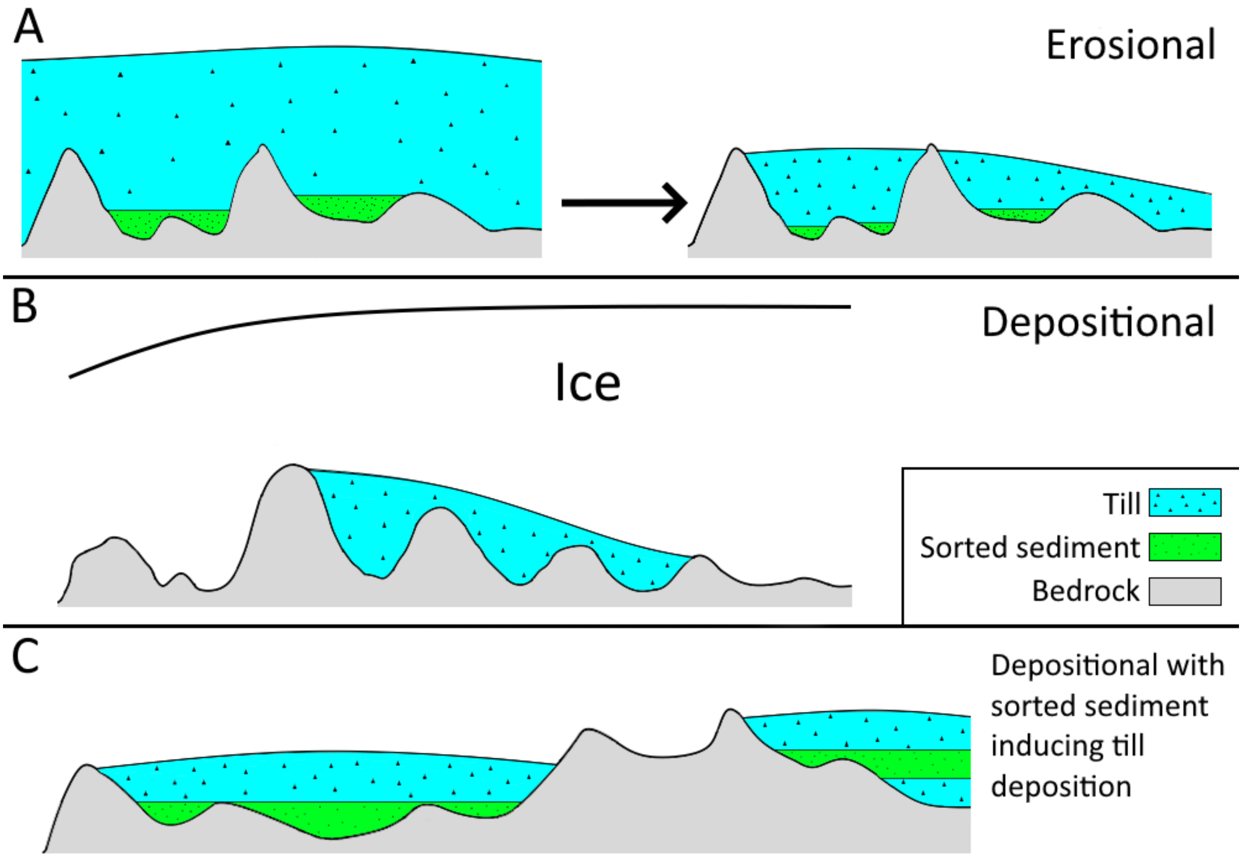

Figure 16. Processes responsible for the formation of subglacial landforms. The landforms are illustrated in a longitudinal profile. (A) Erosional processes where till and sorted sediment have been partially shielded by bedrock from being eroded away entirely. (B) Depositional processes in a hilly terrain where till was deposited and accumulated. (C) Depositional processes in hilly terrain where sorted sediment have induced the deposition of till.

4.5.3 The subglacial flooding theory

An alternative theory of how the drumlins and streamlined till patches may have been formed emphasizes subglacial meltwater flooding as the leading process; named the subglacial flooding theory (e.g. Shaw, 1983; Shaw & Kvill, 1984; Shaw & Sharpe, 1987; Shaw et al., 1989). This theory suggests that drumlins have formed through accumulation of material within cavities aligned with the direction of water movement. These hollows are believed to have been eroded upward into the ice ceiling and subsequently served as sediment traps during decreasing flow. The theory further suggests that the formation of the depositional drumlins may be combined with erosion from vortices by flood water down into the existing material. This results in the drumlins being left behind as erosional remnants. The surrounding material is hence believed to have been eroded away, leaving the drumlins and streamlined till patches upstanding in the landscape.

As subglacial flooding could have contributed to the shape the drumlins and streamlined till patches are shown today, it's difficult to tell the exact influence this process had. The effect the hilly relief terrain may have had on the flooding are also unclear. However, as suggested earlier, the terrain could influence the size of the cavities and thus the amount of material to be trapped within.

5 Conclusions

- Drumlins identified in this study show extensive size (regarding length, width and height) within the landscape in comparison to other drumlins in Sweden and elsewhere (e.g. Clark et al, 2009; Dowling et al., 2015; Möller & Dowling, 2016; Sookhan et al., 2022).

- Nine landforms in this study have been confirmed to be composed of sorted sediment beneath a cover of diamicton, with an additional number identified from previous studies within the study area. The sorted sediment is interpreted to be older than the overlaying diamicton, where the material has been deposited from a previous ice, partly eroded, and shaped by the last glaciation before overlain by a cover of till.

- The distribution between drumlins and streamlined till patches has mainly seemed to coincide, both by comparing drumlins mapped in this study and with drumlins mapped by Dowling et al. (2015).

- Presence of undulated terrain is seen as a main factor for the formation of the mapped drumlins and streamlined till patches, as it may control where material will be accumulated as well as the amount. It is also interpreted that the presence of large, elevated areas (large relative to southern Sweden) could favor accumulation of a greater amount of material.

- Evidence of erosion, as indicated by the presence of older sub-till sediment, meltwater-modified margins, the protective role of bedrock knobs, and the preservation of sediment, underscores processes that could be involved in the formation of drumlins.

- Evidence of deposition is indicated by the presence of till composing the mapped drumlins and streamlined till patches. Also, presence of sorted sediment could have induced the deposition of till, leading to the emplacement of till above the sorted sediment.

References

Alexanderson, H. (2010). Sub-till glaciofluvial sediments at Hultsfred, South Swedish Upland. *GFF, 132* (3–4). Taylor & Francis, 153–159. https://doi.org/10.1080/11035897.2010.508134

Andrén, T., Björck, S., Andrén, E., Conley, D., Zillén, L. & Anjar, J. (2011). The Development of the Baltic Sea Basin During the Last 130 ka. Harff, J., Björck, S. & Hoth, P. (Editors): The Baltic Sea Basin. *Springer, 75–97*. DOI:10.1007/978-3-642-17220-5

Benn, D.I., & Evans, D.J.A. (1996). The interpretation and classification of subglacially deformed-materials. *Quat. Sci. Rev. 15*, 23–52. https://doi.org/10.1016/0277-3791(95)00082-8

Bergström, U., Engdahl, M., Eliasson, T., Ising, J., Girgull, S., Jelinek, C., & Öhrling, C. (2019). *Geologisk beskrivning till utredningsområdet Linköping–Jönköping.* (SGU-rapport 2019:14). Sveriges Geologiska Undersökning.

Blomdin, R., Peterson-Becher, G., Smith, Colby, A., Regnéll, C., Öhrling, C., Goodfellow, Bradley, W., & Mikko, H. (2021). *Beskrivning till geomorfologiska kartan Jämtlands län*. (Serie K, nr 705). Sveriges Geologiska Undersökning.

Boulton, G. (1987). A theory of drumlin formation by subglacial sediment deformation. *Drumlin symposium. p. 25-80*.

Clark, C. D., Hughes, A.L.C., Greenwood, S. L., Spagnolo, M., & Ng, F.S.L. (2009). Size and shape characteristics of drumlins, derived from a large sample, and associated scaling laws. *Quaternary Science Reviews*., 28, 677-69. https://doi.org/10.1016/j.quascirev.2008.08.035

Cohen, K.M., & Gibbard, P.L. (2011). Regional chronostratigraphical correlation table for the last 270,000 years: Europe north of the Mediterranean. In: *INQUA Congress, Bern, 2011.*

Dowling, T.P.F. (2016). *The drumlin problem: streamlined subglacial bedforms in southern Sweden.* [Doctoral Thesis (compilation), Quaternary Sciences]. Department of Geology, Lund University.

Dowling, T.P.F., Spagnolo, M., & Möller, P. (2015). Morphometry and core type of streamlined bedforms in southern Sweden from high resolution LiDAR. *Geomorphology 236*, 54–63. https://doi.org/10.1016/j.geomorph.2015.02.018

Ely, J. C., Clark, C. D., Spagnolo, M., Stokes, C.R., Greenwood, S.L., Hughes, A.L., Dunlop, P., & Hess, D. (2016). Do subglacial bedforms comprise a size and shape continuum? *Geomorphology 257*, 108–119. https://doi.org/10.1016/j.geomorph.2016.01.001

ESRI. (2024). *Minimum Bounding Geometry.* https://desktop.arcgis.com/en/arcmap/latest/tools/data-management-toolbox/minimum-bounding-geometry.htm (Retrieved: 2024-01-03).

Fredén, C. (1983). *Beskrivning till jordartskartan Kungsbacka NO.* (Serie Ae, nr 34). Sveriges Geologiska Undersökning.

Fredholm, K. A. (1875). Några iakttagelser öfver skiktade guslager bland krosstensgrus i Småland. *Geologiska Föreningen i Stockholm Förhandlingar, 2(*12), 522–525. https://doi.org/10.1080/11035897509448101

Gillberg, G. (1955). Den glaciala utvecklingen inom Sydsvenska höglandets västra randzon. *Geol. Fören. Stockh. 77.*

Gillberg, G. (1976). Drumlins in southern Sweden. Bulletin of the Geological Institutions of the University of Uppsala, *New Series, 6*: 125-189.

Green, P. F., Lidmar-Bergström, K., Japsen, P., Bonow, J. M., & Chalmers, J. A. (2013). Stratigraphic landscape analysis, thermochronology and the episodic development of elevated, passive continental margins. *GEUS Bulletin*, *30*, 1–150. https://doi.org/10.34194/geusb.v30.4673

Hart, J. K. (1997). The relationship between drumlins and other forms of subglacial glaciotectonic deformation. Quaternary Science Reviews 16, 93-107. https://doi.org/10.1016/S0277-3791(96)00023-6

Hilldén, A. (1984). *Beskrivning till jordartskartan Borås SO.* (Serie Ae-nr 58). Sveriges Geologiska Undersökning.

Hilldén, A. (1992). *Beskrivning till jordartskartan Ulricehamn SO.* (Serie Ae, nr 109). Sveriges Geologiska Undersökning.

Hilldén, A. (2008). *Beskrivning till jordartskartan 9B Dals-Ed NO*. (Serie K, nr 118). Sveriges Geologiska Undersökning.

Hilldén, A. & Sundevall, S-E. (2010). *Beskrivning till jordartskartan 6C Kinna SV.* (Serie K, nr 260) Sveriges Geologiska Undersökning.

Hillefors, Å. (1974). The stratigraphy and genesis of stoss-and lee-side moraines. Bulletin of the Geological Institutions of the University of Uppsala, *New Series, Vol. 5*, pp. 139-154.

Houmark-Nielsen, M. (2004). The Pleistocene of Denmark: a review of stratigraphy and glaciation history. In: Ehlers, J., Gibbard, P.L. (Editors). *Quaternary Glaciations Extent and Chronology. Part 1: Europe*. (p. 35-46). Developments in Quaternary Science.

Houmark-Nielsen, M. (2010). Extent, age and dynamics of Marine Isotope Stage 3 glaciations in the southwestern Baltic Basin. *Boreas 39*, 343-359. https://doi.org/10.1111/j.1502-3885.2009.00136.x

Houmark-Nielsen, M. (2011). Pleistocene glaciations in Denmark: a closer look at chronology, ice dynamics and landforms. In: Ehlers, J., Gibbard, P.L., Hughes, P.D. (Editors), Quaternary Glaciations e Extent and Chronology. A Closer Look. (p. 47-58). Developments in Quaternary Science.

Hughes, A.L.C., Gyllencreutz, R., Lohne, Ø.S., Mangerud, J. & Svendsen, J.I. (2016). The last Eurasian ice sheets – a chronological database and time-slice reconstruction, DATED-1. *Boreas, 45*(1), 1–45. https://doi.org/10.1111/bor.12142

International Organization for Standardization (ISO). (2017). *Geotechnical investigation and testing Identification and classification of soil*. https://www.iso.org/standard/66345.html (Retrieved: 2024-01-09).

Ising, J. (2012). *Beskrivning till jordartskartan, 7F Tranås SV*. (Serie K, nr 378). Sveriges Geologiska Undersökning.

Ising, J., Bergström, U., Erlström, M., Grigull, S., Malmberg-Persson, K., Wickström, L., Lundqvist, L., & Engdahl, M. (2019). *Hässleholm-Lund-uppgraderad geologisk information inför projektering av höghastighetsjärnväg.* (SGU-rapport 2019:03). Sveriges Geologiska Undersökning.

Iverson, N. R., McCracken, R. G., Zoet, L. K.,Benediktsson, Í. Ö., Schomacker, A., Johnson, M. D., & Woodard, J. (2017). Atheoretical model of drumlin formation based on observations at Múlajökull,Iceland. *Journal of Geophysical Research:Earth Surface,122*, 2302–2323. https://doi.org/10.1002/2017JF004354

Johnson, M. D., Schomacker, A., Benediktsson, Í., Ingólfsson, Ó., Geiger, A., & Ferguson, A. (2010). Active drumlin field revealed at the margin of Mulajokull, Iceland: A surge-type glacier. *Geology*, *38(10)*, 943–946. https://doi.org/10.1130/G31371.1

Karlsson, C., Sohlenius, G., & Peterson-Becher, G. (2021). *Handledning för jordartsgeologiska kartor och databaser över Sverige.* (SGU-rapport 2021:17). Sveriges geologiska undersökning, 83 s.

Kleman, J. (1994). Preservation of landforms under ice sheets and ice caps. *Geomorphology 9*, 19-32. https://doi.org/10.1016/0169-555X(94)90028-0

Kleman, J., & Glasser, N.F. (2007). Subglacial Thermal Organization (STO) of Ice Sheets. *Quat. Sci. Rev. 26*, 585-597. https://doi.org/10.1016/j.quascirev.2006.12.010

Kleman, J., Hättestrand, M., Borgström, I., Fabel, D., & Preusser, F. (2021). Age and duration of a MIS 3 interstadial in the Fennoscandian Ice Sheet core area–Implications for ice sheet dynamics. *Quaternary Science Reviews, 264*, 107011. https://doi.org/10.1016/j.quascirev.2021.107011

Kleman, J., & Stroeven, A.P. (1997). Preglacial surface remnants and Quaternary glacial regimes in north-western Sweden. *Geomorphology 19*, 35-54. https://doi.org/10.1016/S0169-555X(96)00046-3

Lagerbäck, R. (1988). The Veiki moraines in northern Sweden- widespread evidence of an Early Weichselian deglaciation. *Boreas 17*, 469-486. https://doi.org/10.1111/j.1502-3885.1988.tb00562.x

Lagerbäck, R. (2018). Den senaste nedisningen i södra Sverige – och tiden dessförinnan. *Rapporter och meddelanden 143*. Sveriges geologiska undersökning, 92.

Lantmäteriet. (2020). *Quality Description- National Elevation Model.* https://www.lantmateriet.se/globalassets/geodata/geodataprodukter/hojddata/quality_description_dtm.pdf (Retrieved: 2024-01-03).

Lantmäteriet. (2024). *Öppna data.* https://www.lantmateriet.se/sv/geodata/vara-produkter/oppna-data/ (Retrieved: 2024-04-02).

Larsen, N.K., Knudsen, K.L., Krohn, C.F., Kronborg, C., Murray, A.S., & Nielsen, O.B. (2009a). Late Quaternary ice sheet, lake and sea history of southwestern Scandinavia- a synthesis. *Boreas 38*, 732-761. http://dx.doi.org/10.1111/j.1502-3885.2009.00101.x

Larsen, N.K., Krohn, C.F., Kronborg, C., Nielsen, O.B., & Knudsen, K.L. (2009b). Litostratigraphy of the Late Saalian to Middle Weichselian Skærumshede Group in Vendsyssel, northern Denmark. Boreas 38, 762-786. https://doi.org/10.1111/j.1502-3885.2009.00102.x

Lewington, E., Livingstone, S., Sole, A., Clark, C., & Ng, F.S.L. (2019). An automated method for mapping geomorphological expressions of former subglacial meltwater pathways (hummock corridors) from high resolution digital elevation data. *Geomorphology. 339. https://doi.org/10.1016/j.geomorph.2019.04.013*

Lidmar-Bergström, K. (1988). Denudation surfaces of a shield area in south Sweden. Geografiska Annaler 70A, 337–350. https://doi.org/10.2307/521267

Lidmar-Bergström, K. (2009). Berggrundens ytformer. Fredén C. (Editor). (p. 44-54). *Berg och jord*. Sveriges Nationalatlas.

Lidmar-Bergström, K., & Näslund J. O. (2002). Landforms and uplift in Scandinavia. *Geological Society, London, Special Publications 196*, 103–116. https://doi.org/10.1144/gsl.sp.2002.196.01.07

Lidmar-Bergström, K., Olvmo, M., & Bonow, J, M. (2017). The South Swedish Dome: a key structure for identification of peneplains and conclusions on Phanerozoic tectonics of an ancient shield. *GFF, 139:4*, 244-259, https://doi.org/10.1080/11035897.2017.1364293

López, G. (2016). Grain size analysis. In: Gilbert AS (ed) Encyclopedia of Geoarchaeology. *Springer, Berlin,* pp 341–348.

Lundqvist, J. (2009). Weichsel-istidens huvudfas. Fredén C. (Editor). (p. 124-135). *Berg och jord*. Sveriges Nationalatlas.

Mangerud, J. (2021). The discovery of the Younger Dryas, and comments on the current meaning and usage of the term. Boreas, Vol. 50, pp. 1–5. https://doi.org/10.1111/bor.12481

Menzies, J. (1979). A review of the literature on the formation and location of drumlins. *Earth-Science Reviews 14,* 315–359. https://doi.org/10.1016/0012-8252(79)90093-X

Möller, P. (2010). Sub-till sediments on the Småland peneplain: their age, and implications for south-Swedish glacial stratigraphy and glacial dynamics*. Lundqua Report. (Vol. 40)*. Department of Geology, Lund University.

Möller, P., Alexanderson, H., Anjar, J., & Björck, S. (2020). MIS 3 sediment stratigraphy in southern Sweden sheds new light on the complex glacial history and dynamics across southern Scandinavia. *Boreas, 49*(3), 389–416. https://doi.org/10.1111/bor.12433

Möller, P., & Dowling, T.P.F. (2016). Streamlined subglacial bedforms on the Närke plain, south-central Sweden – Areal distribution, morphometrics, internal architecture and formation. *Quat. Sci. Rev. 146,* 182–215. https://doi.org/10.1016/j.quascirev.2016.04.007

Möller, P., & Dowling, T.P.F. (2018). Equifinality in glacial geomorphology: instability theory examined via ribbed moraine and drumlins in Sweden, *GFF, 140:2*, 106-135, https://doi.org/10.1080/11035897.2018.1441903

Möller, P., & Murray, A.S. (2015). Drumlinised glaciofluvial and glaciolacustrine sediments on the Småland peneplain, South Sweden – new information on the growth and decay history of the Fennoscandian Ice Sheets during MIS 3. *Quat. Sci. Rev. 122*, 1–29. https://doi.org/10.1016/j.quascirev.2015.04.025

Napieralski, J., & Nalepa, N. (2010). The application of control charts to determine the effect of grid cell size on landform morphometry. *Comput. Geosci. 36* (2), 222–230. https://doi.org/10.1016/j.cageo.2009.06.003

Newcastle University. (2024a). Strength of Correlation. https://www.ncl.ac.uk/webtemplate/ask-assets/external/maths-resources/statistics/regression-and-correlation/strength-of-correlation.html (Retrieved: 2024-04-09).

Newcastle University. (2024b). Introduction to Hypothesis Testing and Confidence Intervals (Animal Science). https://www.ncl.ac.uk/webtemplate/ask-assets/external/maths-resources/animal-science/hypothesis-tests/introduction-to-hypothesis-testing-and-confidence-intervals.html (Retrieved: 2024-04-09).

Nordenskjöld, C.E. (1944). Morfologiska studier inom övergångsområdet mellan Kalmarslätten och Tjust. *Medd. Lunds Univ. Geogr. Inst. Avh. VIII. 21*.

Olvmo, M., Lidmar-Bergström, K., Ericson, K. & Bonow, J. (2005). Saprolite remnants as indicators of pre-glacial landform genesis in southeast Sweden. *Geografiska Annaler 87A,* 447–460. https://doi.org/10.1111/j.0435-3676.2005.00270.x

Paint.NET. (2024). *Home*. https://www.getpaint.net (Retrieved: 2024-04-24).

Peterson-Becher, G., & Johnson, M., D. (2018). Hummock corridors in the south-central sector of the Fennoscandian ice sheet, morphometry and pattern. *Earth Surface Processes and Landforms 43*, 919–929. https://doi.org/10.1002/esp.4294

Peterson-Becher, G., Johnson, M., D., & Smith C. A. (2017). Glacial geomorphology of the south Swedish uplands – focus on the spatial distribution of hummock tracts. *Journal of Maps, 13:2*, 534-544. https://doi.org/10.1080/17445647.2017.1336121

Perhans, K-E. (2002). Istidens landskap: jordarter och terrängformer. Sollentuna: Geo läromedel. ISBN:919740442X

Påsse, T. (1988). Beskrivning av jordartskartan- Varberg SO/ Ullared SV. (Serie Ae, nr 86). Sveriges Geologiska Undersökning.

Påsse, T. (1993). *Beskrivning till jordartskartan Ullared SO.* (Serie Ae, nr 115). Sveriges Geologiska Undersökning.

Regnell, C., Mangerud, J. & Svendsen, J. I. (2019). Tracing the last remnants of the Scandinavian Ice Sheet: Ice-dammed lakes and a catastrophic outburst flood in northern Sweden, *Quaternary Science Reviews, 221*, 105862 s. https://doi.org/10.1016/j.quascirev.2019.105862

Rudberg, S. (1960). Geology and geomorphology. In: Sømme A, (Editor). (p. 27–40). *A geography of Norden*. Cappelen forlag.

Shaw, J. (1983). Drumlin formation related to inverted melt-water erosional marks. *Journal of Glaciology 29*, 461–479. https://doi.org/10.3189/S0022143000030367

Shaw, J., & Kvill, D. (1984). A glaciofluvial origin for drumlins of the Livingstone Lake area, Saskatchewan. *Canadian Journal of Earth Sciences 21*, 1442–1459. https://doi.org/10.1139/e84-150

Shaw, J., Kvill, D. & Rains, B. (1989). Drumlins and catastrophic subglacial floods. *Sedimentary Geology, 62*, 177-202. https://doi.org/10.1016/0037-0738(89)90114-0

Shaw, J., & Sharpe, D. R. (1987). Drumlin formation by subglacial meltwater erosion. *Canadian Journal of Earth Sciences 24*, 2316–2322. https://doi.org/10.1139/e87-216

Sookhan, S., Eyles, N., & Bukhari, S. (2022). Drumlins and mega-scale glacial lineations as a continuum of subglacial shear marks: A LiDAR based morphometric study of streamlined surfaces on the bed of a Canadian paleo-ice stream. *Quaternary Science Reviews. 292.* https://doi.org/10.1016/j.quascirev.2022.107679

Spagnolo, M., Clark, C.D., & Hughes, A.L.C. (2012). Drumlin relief. *Geomorphology, 153–154,* 179–191. https://doi.org/10.1016/j.geomorph.2012.02.023

Spagnolo, M., Clark, C.D., Hughes, A.L.C., Dunlop, P., & Stokes, C.R. (2010). The planar shape of drumlins. *Sedimentary Geology 232*, 119-129. https://doi.org/10.1016/j.sedgeo.2010.01.008+%7C

Statens Meteorologisk-Hydrografiska Anstalt. (1928). Förteckning över Sveriges vattenfall. *H. 34,* Gideälv. (Kartblad 136-138).

Stokes, C.R., Spagnolo, M., & Clark, C.D. (2011). The composition and internal structure of drumlins: Complexity, commonality, and implications for a unifying theory of their formation. *Earth Science Reviews 107*, 398-422. https://doi.org/10.1016/j.earscirev.2011.05.001

Stokes, C. R., Fowler, A. C., Clark, C. D., Hindmarsh, R.C.A., & Spagnolo, M. (2012). The instability theory of drumlin formation and its explanation of their varied composition and internal structure. *Quaternary Science Reviews 62*, 77–96. https://doi.org/10.1016/j.quascirev.2012.11.011

Strahler, A., & Strahler A. (2004). *Physical Geography- Science and Systems of the Human Environment.* (3:rd edition). John Wiley & Sons.

Stroeven, A.P., Hättestrand, C., Kleman, J., Heyman, J., Fabel, D., Fredin, O., Goodfellow, B.W., Harbor, J.M., Jansen, J.D., Olsen, L., Caffee, M.W., Fink, D., Lundqvist, J., Rosqvist, G.C., Strömberg, B., & Jansson, K.N. (2016). Deglaciation of Fennoscandia. *Quaternary Science Reviews, 147*, 91–121. https://doi.org/10.1016/j.quascirev.2015.09.016

Sundevall, S-E. (2006). *Beskrivning till jordartsgeologiska kartan 6D Gislaved SV.* (Serie K, nr 65). Sveriges Geologiska Undersökning.

Svantesson, S. I. (2001). *Beskrivning till jordartskartan 6F Vetlanda NV*. (Serie Ae, Nr 146). Sveriges Geologiska Undersökning.

Svenska Akademiens ordbok (SAOB). (2024). *Morän*. https://www.saob.se/artikel/?unik=M_1261-0427.3VYm. (Retrieved: 2024-02-25).

Sveriges Geologiska Undersökning (SGU). (2019). *Öppna data.* https://www.sgu.se/produkter-och-tjanster/geologiska-data/oppna-data/ (Retrieved: 2024-04-02).

Sveriges Geologiska Undersökning. (SGU). (2020a). *Isen smälter.* https://www.sgu.se/om-geologi/jord/fran-istid-till-nutid/isen-smalter/ (Retrieved: 2023-12-05).

Sveriges Geologiska Undersökning (SGU). (2020b). *Morän- spår av inlandsisen*. https://www.sgu.se/om-geologi/jord/fran-istid-till-nutid/inlandsisen/moran-spar-av-inlandsisen/ (Retrieved: 2024-02-06).

Sveriges Geologiska Undersökning, (SGU). (2024a). *Kartvisaren Jordlagerföljder.* https://www.sgu.se/produkter-och-tjanster/kartor/kartvisaren/jordkartvisare/jordlagerfoljder/ (Retrieved: 2024-01-04).

Sveriges Geologiska Undersökning. (SGU). (2024b). *Jordarter 1:25000 -1:100000.* https://apps.sgu.se/kartvisare/kartvisare-jordarter-25-100.html (Retrieved: 2024-02-15).

Sveriges lantbruksuniversitet (SLU). (2024). *Geodata Extraction Tool*. https://herkules.slu.se/get/ (Retrieved: 2024-01-03).

Tamm, G. (1925). *Grundvattenrörelser och försupningsprocesser belysta genom bestämningar av grundvattnets syrehalt i nordsvenska moräner.* (Nr. 22). Statens Skogsförsöksanstalt.

Tamm, G. (1931). *Studier över jordmånstyper och deras förhållande till markens hydrologi i nordsvenska skogsterränger.* (Nr. 26). Statens Skogsförsöksanstalt.

University of Kentucky. (2024). *Science Sleuths: the Science that Shapes Diagnostic Tests: What Does 'Statistically Significant' Actually Mean?* https://equine.ca.uky.edu/content/what-does-%E2%80%98statistically-significant%E2%80%99-actually-mean (Retrieved: 2024-04-18).

University of Sheffield (TUOS). (2024a). *Drumlins*. https://www.sheffield.ac.uk/drumlins/definition (Retrieved: 2024-03-05).

University of Sheffield (TUOS). (2024b). *Crag and Tail*. https://www.sheffield.ac.uk/drumlins/cragandtail (Retrieved: 2024-03-05).

Vatteninformationssystem Sverige (VISS). (2023). Geografisk Region. https://visshjalp.lansstyrelsen.se/detta-beskrivs-i-viss/allmanna-uppgifter-grundvatten/geografisk-region/ (Retrieved: 2023-12-19).

Vikberg-Samuelsson, E., Peterson-Becher, G., & Leroux, Virginie. (2022). *Lidmoränen i Berg och dess potential som grundvattenmagasin.* (SGU-rapport 2022:07). Sveriges Geologiska Undersökning.

Öhrling, C., Peterson, G., & Johnson, M. D. (2020). Glacial geomorphology between Lake Vänern and Lake Vättern, southern Sweden. Journal of Maps, 16:2, 776-789, DOI:10.1080/17445647.2020.1820386

Appendix

Appendix 1. Coordinates for each visited site.

Site	X	Y
1.1	339608	6383551
1.2	339616	6383554
1.3	339628	6383557
1.4	339632	6383533
1.5	339705	6383584
2.1	341869	6384721
2.2	342361	6385449
2.3	342699	6385672
3	346425	6388961
4.1	352095	6392457
4.2	352102	6392421
5.1	350256	6374750
5.2	350161	6374664
6.1	357898	6377544
6.2	357894	6377557
6.3	357910	6377547
6.4	357893	6377569
7	356631	6368793
8	361300	6373227
9	395255	6362382
10.1	400391	6375126
10.2	400358	6375107
11	385067	6385694
12.1	384748	6385986
12.2	384736	6385985
13.1	381992	6388647
13.2	381982	6388650
13.3	381987	6388675
13.4	381978	6388680

Appendix 2. Protocol for sieving of diamicton.

Protocol for sieving diamicton (for '500 g' sample)

Date ______________________________________

Sample mass ('500 g sample') before wet-sieving ____________________ **g**

Sample mass ('500 g sample') after wet-sieving__________________ **g**

% fine material wet.seived away ________________________

Sieve, mm	Mass, g	Mass, %	Cumulative weight, %
<0,063			
0,063			
0,125			
0,25			
0,5			
1			
2			
4			
8			
16			
TOTAL			

TOTAL >0,063	

Appendix 3. Protocol for hydrometer test of diamicton.

Protocol for hydrometer of diamicton ('100 g' sample)

Date ______________________________

Diamicton mass ____________________ **g**

Beaker mass _____________________ **g**

Beaker plus dried sediment _________________ **g**

Dried sediment ___________________________ **g**

Hydrometer reading for the diamicton

At the appointed time, read off the scale on the hydrometer. Write down the corresponding grain size from the nomogram on the next page.

Sedimentation time, minutes	Grain size indicated on nomogram	g/l (from hydrometer)	% diamicton less than measured grain size
0,5			
1			
2			
4			
10			
20			
50			
100			
200			
400			
Ca 1440			

Appendix 4

Sieve Analysis

After each sample was weighed to the set weight, 500 g, they were dry sieved by hand using a 2 mm sieve. Material above 2 mm was placed in separate foil forms, whereas material below 2 mm was placed in large beakers together with 100 ml 0.05 M Na6P6O18 (Sodium hexametaphosphate) and 500 ml of distilled water. Each sample was vigorously stirred for 10 min. The samples were then wet sieved through a 0.063 mm sieve using distilled water, until the water running out the sieve was clear. A hand lens was also used to observe when the sediments were clean of particles <O.063 mm. After this, the sediments left in the sieve were put into foil forms together with the material above 2 mm and placed into an oven to dry overnight. Each sample was in the oven for 24 h at 105°C.

The day after, the samples were weighed once more. This was made in order to calculate the percentage of material washed away. Each sample was then dry sieved in a sieve shaker using the 16, 8, 4, 2, 1.4, 1, 0.71, 0.5, 0.355, 0.250, 0.180, 0.125, 0.09 and 0.063 mm sieves. Each sample was shaken for 10 min. The material within each sieve was then weighed. The weight percentage for each fraction could thus be calculated. The cumulative weight was calculated by successively subtracting the weight percentage of each fraction, starting at 100%. This process commenced with the largest fraction (16 mm) and proceeded in a descending order. Material <0.063 mm was calculated by subtracting the total mass before the dry sieving with the total mass after the dry sieving.

Hydrometer Analysis

100 g from each sample was dry sieved by hand using a 2 mm sieve, discarding particles exceeding 2 mm. Each sample was then placed in a 1000 ml cylinder together with 100 ml 0,05 M Na6P6O18 (Sodium hexametaphosphate) and 300 ml of distilled water, and vigorously stirred for 10 min. The 1000 ml cylinders were then filled up with distilled water and stirred once again. A hydrometer was placed in each of the cylinders and was read off at 0.5 min, 1 min, 2 min, 4 min, 10 min, 20 min, 50 min, 100 min (1 h 40 min), 200 min (3 h 20 min), 400 min (6 h 40 min) and 1440 min (24 h). The unit used on the hydrometer was g/l. By plotting the time of reading against the corresponding read values (in g/l) on a nomogram, the grain size could be determined. Figure 1 shows the nomogram used.

The next day, the last reading was noted. After this, each sample was wet sieved through a 0.063 mm sieve and then oven dried for 24 h at 105°C. The samples were put in foil forms before being placed in the oven. After drying, the samples were weighed, as well as the empty foil form in order to calculate the amount of material within each form. The weight percentage of each fraction could thus be calculated, as well as determining each cumulative weight. The latter was calculated by dividing the read value from the hydrometer with the sample weight before the hydrometer analysis. The cumulative values obtained from this analysis were combined with those determined through the Sieve Analysis of the same sample, creating a cumulative frequency curve for all grain sizes. This was made for all the eight samples respectively.

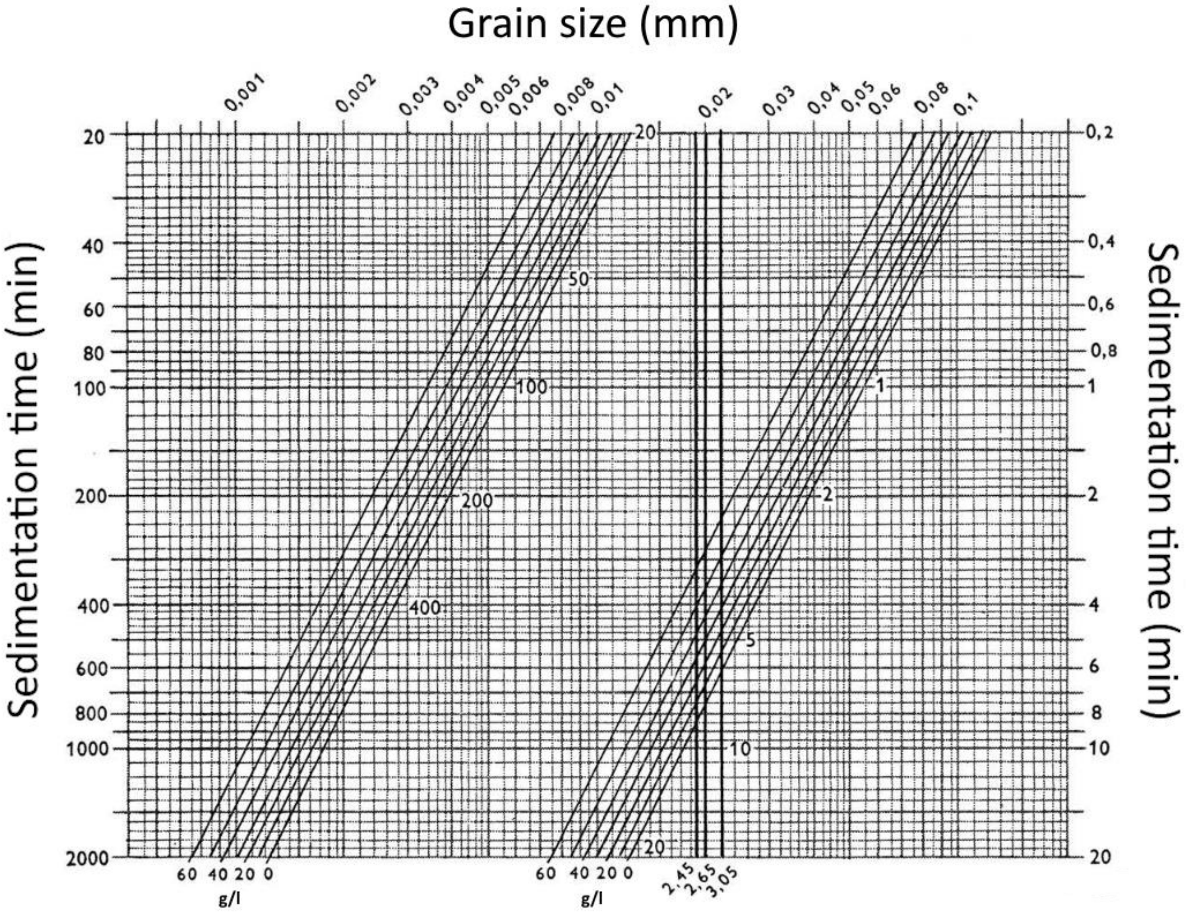

Figure 1. Nomogram used to determine the grain size (modified from Gandahl, 1952).

Appendix 5. Additional information for table 3 showing what type of observation that was conducted, the end and coordinates.

Landform	Database-ID	Type of observation	End	N	E
A	BMW030072	Drilling/ Prode; machine driven	Likely to bedrock	6409346	489793
	BMW030072	Drilling/ Prode; machine driven	Likely to bedrock	6409346	489793
	BMW030072	Drilling/ Prode; machine driven	Likely to bedrock	6409346	489793
	BMW030072	Drilling/ Prode; machine driven	Likely to bedrock	6409346	489793
B	ELM082032	Drilling/ Prode; machine driven	To bedrock	6326596	482173
	ELM082032	Drilling/ Prode; machine driven	To bedrock	6326596	482173
	ELM082032	Drilling/ Prode; machine driven	To bedrock	6326596	482173
	ELM082032	Drilling/ Prode; machine driven	To bedrock	6326596	482173
C	EDA990064	Cut in terrain; machine- dug pit	In the same layer (open end)	6375586	488410
	EDA990064	Cut in terrain; machine- dug pit	In the same layer (open end)	6375586	488410
	EDA990064	Cut in terrain; machine- dug pit	In the same layer (open end)	6375586	488410
D	SIS980170	Drilling/ Prode; machine driven	Not classified	6373926	505134
	SIS980170	Drilling/ Prode; machine driven	Not classified	6373926	505134
E	BMW188093	Cut in terrain; machine- dug pit	In the same layer (open end)	6426926	491116
	BMW188093	Cut in terrain; machine- dug pit	In the same layer (open end)	6426926	491116
	BMW188093	Cut in terrain; machine- dug pit	In the same layer (open end)	6426926	491116
	CHO182001	Wall in a excavation pit; unspecified	In debris (open end)	6428250	492552
	CHO182001	Wall in a excavation pit; unspecified	In debris (open end)	6428250	492552
	CHO182001	Wall in a excavation pit; unspecified	In debris (open end)	6428250	492552
	CHO182001	Wall in a excavation pit; unspecified	In debris (open end)	6428250	492552
F	EDA901011	Drilling/ Prode; machine driven	To bedrock	6181392	410099
	EDA901011	Drilling/ Prode; machine driven	To bedrock	6181392	410099
	EDA901011	Drilling/ Prode; machine driven	To bedrock	6181392	410099
G	GRD082003	Cut in terrain; pit	In the same layer (open end)	6425336	507063
	GRD082003	Cut in terrain; pit	In the same layer (open end)	6425336	507063
	GRD082006	Cut in terrain; pit	In debris (open end)	6425227	507661
	GRD082006	Cut in terrain; pit	In debris (open end)	6425227	507661
	JIG112102	Drilling/ Prode; machine driven	In the same layer (open end)	6424529	507589
	JIG112102	Drilling/ Prode; machine driven	In the same layer (open end)	6424529	507589
	JIG112102	Drilling/ Prode; machine driven	In the same layer (open end)	6424529	507589
	JIG112102	Drilling/ Prode; machine driven	In the same layer (open end)	6424529	507589
	JIG112102	Drilling/ Prode; machine driven	In the same layer (open end)	6424529	507589
	JIG112103	Drilling/ Prode; machine driven	To block or bedrock	6424498	508112
	JIG112103	Drilling/ Prode; machine driven	To block or bedrock	6424498	508112
H	EDA082018	Cut in terrain; machine- dug pit	In the same layer (open end)	6289984	473261
	EDA082018	Cut in terrain; machine- dug pit	In the same layer (open end)	6289984	473261
	EDA082019	Cut in terrain; machine- dug pit	In the same layer (open end)	6291082	473059
	EDA082019	Cut in terrain; machine- dug pit	In the same layer (open end)	6291082	473059
	EDA082019	Cut in terrain; machine- dug pit	In the same layer (open end)	6291082	473059
	EDA082020	Cut in terrain; machine- dug pit	In the same layer (open end)	6291847	473236
	EDA082020	Cut in terrain; machine- dug pit	In the same layer (open end)	6291847	473236
	EDA082020	Cut in terrain; machine- dug pit	In the same layer (open end)	6291847	473236

Appendix 6.A. Raw data from grain size analysis, showing data from sieving- and hydrometer analysis for sample 1.6. The table on the left is from the sieve analysis and the table on the right is from the hydrometer analysis.

Sieving (mm)	Weight (g)	Precental weight (%)	Cumulative weight (%)
16	0	0	100
8	43.5	8.7	91.3
4	49.8	10.0	81.3
2	48.5	9.7	71.6
1.4	28.7	5.7	65.9
1	28.4	5.7	60.2
0.71	31.7	6.3	53.9
0.5	39.0	7.8	46.1
0.355	43.6	8.7	37.4
0.25	37.7	7.5	29.8
0.18	19.5	3.9	25.9
0.125	24.7	4.9	21.0
0.09	11.0	2.2	18.8
0.063	6.9	1.4	17.4
<0.063	85.9	17.2	0.2
Total weight	498.9	99.8	

Time (min)	Grain size indicated on nomogram (mm)	Cumulative weight (%)
0.5	0.07	18.0
1	0.052	14.0
2	0.036	9.5
4	0.027	6.5
10	0.017	5.2
20	0.02	4.5
50	0.0075	4.2
100	0.0054	4,0
200	0.0039	3.7
400	0.0027	3.6
1440	0.00145	3.5

Appendix 6.B. Raw data from grain size analysis, showing data from sieving- and hydrometer analysis for sample 3. The table on the left is from the sieve analysis and the table on the right is from the hydrometer analysis.

Sieving (mm)	Weight (g)	Precental weight (%)	Cumulative weight (%)
16	0	0	100
8	27.0	5.4	94.6
4	35.9	7.2	87.4
2	34.3	6.9	80.6
1.4	18.6	3.7	76.8
1	19.6	3.9	72.9
0.71	20.6	4.1	68.8
0.5	26.5	5.3	63.5
0.355	32.2	6.4	57.1
0.25	38.6	7.7	49.3
0.18	21.8	4.4	45.0
0.125	44.3	8.9	36.1
0.09	31.5	6.3	29.8
0.063	20.0	4.0	25.8
<0.063	128.0	25.6	0.2
Total weight	498.9	99.8	

Time (min)	Grain size indicated on nomogram (mm)	Cumulative weight (%)
0.5	0.068	26.5
1	0.049	21.2
2	0.035	17.3
4	0.0245	15.3
10	0.016	12.1
20	0.0118	9.5
50	0.0075	6.1
100	0.054	5.0
200	0.0039	4.6
400	0.0027	4.4
1440	0.00145	4.1

Appendix 6.C. Raw data from grain size analysis, showing data from sieving- and hydrometer analysis for sample 4.1. The table on the left is from the sieve analysis and the table on the right is from the hydrometer analysis.

Sieving (mm)	Weight (g)	Precental weight (%)	Cumulative weight (%)
16	0	0	100
8	25.6	5.1	94.9
4	54.0	10.8	84.1
2	48.4	9.7	74.4
1.4	15.3	3.1	71.3
1	20.4	4.1	67.3
0.71	22.7	4.5	62.7
0.5	28.6	5.7	57.0
0.355	34.2	6.8	50.2
0.25	38.0	7.6	42.6
0.18	54.6	10.9	31.6
0.125	29.0	5.8	25.8
0.09	10.5	2.1	23.7
0.063	6.7	1.3	22.4
<0.063	110.7	22.1	0.3
Total weight	498.7	99.7	

Time (min)	Grain size indicated on nomogram (mm)	Cumulative weight (%)
0.5	0.066	23.0
1	0.049	19.0
2	0.035	14.9
4	0.0245	13.1
10	0.016	11.2
20	0.0118	9.5
50	0.0074	7.8
100	0.0053	6.6
200	0.0038	6,0
400	0.0025	5.8
1440	0.00143	5.6

Appendix 6.D. Raw data from grain size analysis, showing data from sieving- and hydrometer analysis for sample 4.2. The table on the left is from the sieve analysis and the table on the right is from the hydrometer analysis.

Sieving (mm)	Weight (g)	Precental weight (%)	Cumulative weight (%)
16	0	0	100
8	27.3	5.5	94.5
4	21.4	4.3	90.3
2	41.6	8.3	81.9
1.4	11.9	2.4	79.6
1	15.9	3.2	76.4
0.71	17.9	3.6	72.8
0.5	21.6	4.3	68.5
0.355	27.4	5.5	63.0
0.25	34.2	6.8	56.2
0.18	35.3	7.1	49.1
0.125	68.5	13.7	35.4
0.09	16.8	3.4	32.0
0.063	10.6	2.1	29.9
<0.063	147.0	29.4	0.5
Total weight	497.4	99.5	

Time (min)	Grain size indicated on nomogram (mm)	Cumulative weight (%)
0.5	0.064	30.0
1	0.048	23.5
2	0.034	19.2
4	0.0235	15.4
10	0.01575	12.7
20	0.0118	10.2
50	0.0074	7.7
100	0.0053	5.5
200	0.0038	5.0
400	0.0026	4.6
1440	0.00144	4.5

Appendix 6.E. Raw data from grain size analysis, showing data from sieving- and hydrometer analysis for sample 6.1. The table on the left is from the sieve analysis and the table on the right is from the hydrometer analysis.

Sieving (mm)	Weight (g)	Precental weight (%)	Cumulative weight (%)
16	0	0	100
8	26.5	5.3	94.7
4	39.4	7.9	86.8
2	44.9	9.0	77.8
1.4	25.1	5.0	72.8
1	31.9	6.4	66.4
0.71	34.8	7.0	59.5
0.5	36.0	7.2	52.3
0.355	36.5	7.3	45.0
0.25	37.0	7.4	37.6
0.18	46.0	9.2	28.4
0.125	26.8	5.4	23.0
0.09	15.5	3.1	19.9
0.063	9.5	1.9	18.0
<0.063	87.7	17.5	0.5
Total weight	497.6	99.5	

Time (min)	Grain size indicated on nomogram (mm)	Cumulative weight (%)
0.5	0.07	18.5
1	0.051	15.0
2	0.036	11.5
4	0.026	8.5
10	0.0165	7.7
20	0.0118	7.3
50	0.0074	6.1
100	0.0053	5.5
200	0.0038	4.8
400	0.0027	4.4
1440	0.00144	4.2

Appendix 6.F. Raw data from grain size analysis, showing data from sieving- and hydrometer analysis for sample 6.3. The table on the left is from the sieve analysis and the table on the right is from the hydrometer analysis.

Sieving (mm)	Weight (g)	Precental weight (%)	Cumulative weight (%)
16	0	0	100
8	2.4	0.5	99.5
4	1.2	0.2	99.3
2	1.5	0.3	99.0
1.4	1.0	0.2	98.8
1	2.1	0.4	98.4
0.71	2.7	0.5	97.8
0.5	3.1	0.6	97.2
0.355	4.6	0.9	96.3
0.25	23.2	4.6	91.6
0.18	54.4	10.9	80.8
0.125	142.9	28.6	52.2
0.09	108.2	21.6	30.5
0.063	24.8	5.0	25.6
<0.063	125.9	25.2	0.4
Total weight	498.0	99.6	

Time (min)	Grain size indicated on nomogram (mm)	Cumulative weight (%)
0.5	0.066	26.0
1	0.047	21.0
2	0.034	17.0
4	0.024	14.5
10	0.01575	12.0
20	0.0117	11.5
50	0.0072	8.3
100	0.0053	7.4
200	0.0037	6.7
400	0.0025	6.1
1440	0.00143	5.9

Appendix 6.G. Raw data from grain size analysis, showing data from sieving- and hydrometer analysis for sample 6.4. The table on the left is from the sieve analysis and the table on the right is from the hydrometer analysis.

Sieving (mm)	Weight (g)	Precental weight (%)	Cumulative weight (%)
16	0	0	100
8	14.6	2.9	97.1
4	31.6	6.3	90.8
2	32.3	6.5	84.3
1.4	11.3	2.3	82.0
1	16.0	3.2	78.8
0.71	19.5	3.9	74.9
0.5	25.2	5.0	69.9
0.355	32.1	6.4	63.5
0.25	36.6	7.3	56.2
0.18	57.9	11.6	44.6
0.125	49.6	9.9	34.7
0.09	9.7	1.9	32.7
0.063	11.5	2.3	30.4
<0.063	150.6	30.1	0.3
Total weight	498.5	99.7	

Time (min)	Grain size indicated on nomogram (mm)	Cumulative weight (%)
0.5	0.064	30.5
1	0.047	24.5
2	0.034	19.7
4	0.0235	16.0
10	0.01575	12.6
20	0.0118	9.2
50	0.0074	6.8
100	0.0053	5.7
200	0.0038	4.9
400	0.0027	4.3
1440	0.00144	4.2

Appendix 6.H. Raw data from grain size analysis, showing data from sieving- and hydrometer analysis for sample 9. The table on the left is from the sieve analysis and the table on the right is from the hydrometer analysis.

Sieving (mm)	Weight (g)	Precental weight (%)	Cumulative weight (%)
16	0	0	100
8	6.5	1.3	98.7
4	27.8	5.6	93.1
2	39.5	7.9	85.2
1.4	6.8	1.4	83.9
1	10.8	2.2	81.7
0.71	13.8	2.8	79.0
0.5	19.5	3.9	75.1
0.355	27.2	5.4	69.6
0.25	35.7	7.1	62.5
0.18	58.1	11.6	50.9
0.125	56.0	11.2	39.7
0.09	24.7	4.9	34.7
0.063	18.6	3.7	31.0
<0.063	153.7	30.7	0.3
Total weight	498.7	99.7	

Time (min)	Grain size indicated on nomogram (mm)	Cumulative weight (%)
0.5	0.063	31.0
1	0.047	25.0
2	0.034	20.9
4	0.0245	17.0
10	0.01575	13.8
20	0.0117	12.0
50	0.0072	9.8
100	0.0052	8.7
200	0.0037	7.4
400	0.0025	5.8
1440	0.00143	5.2

Appendix 7.A. Core logs from Möller et al. (2020), showing the sampling sites of Kronobergshed (A) and Upplid (B).

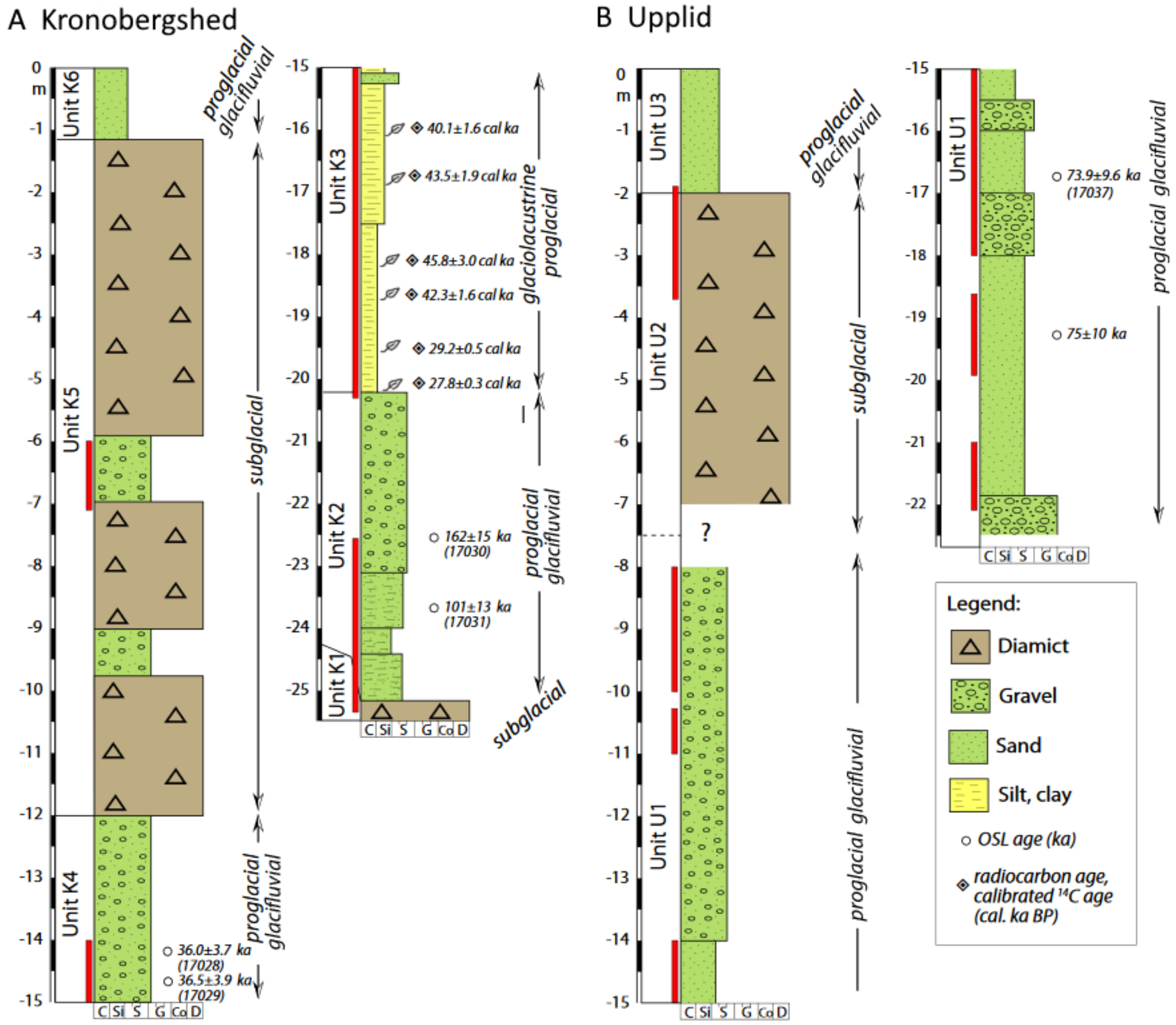

Appendix 7.B. Core logs from Möller et al. (2020, left) and Möller and Murray (2015, right), showing the sampling sites of Tunatorp Södergård (A) and Grännafors (B).

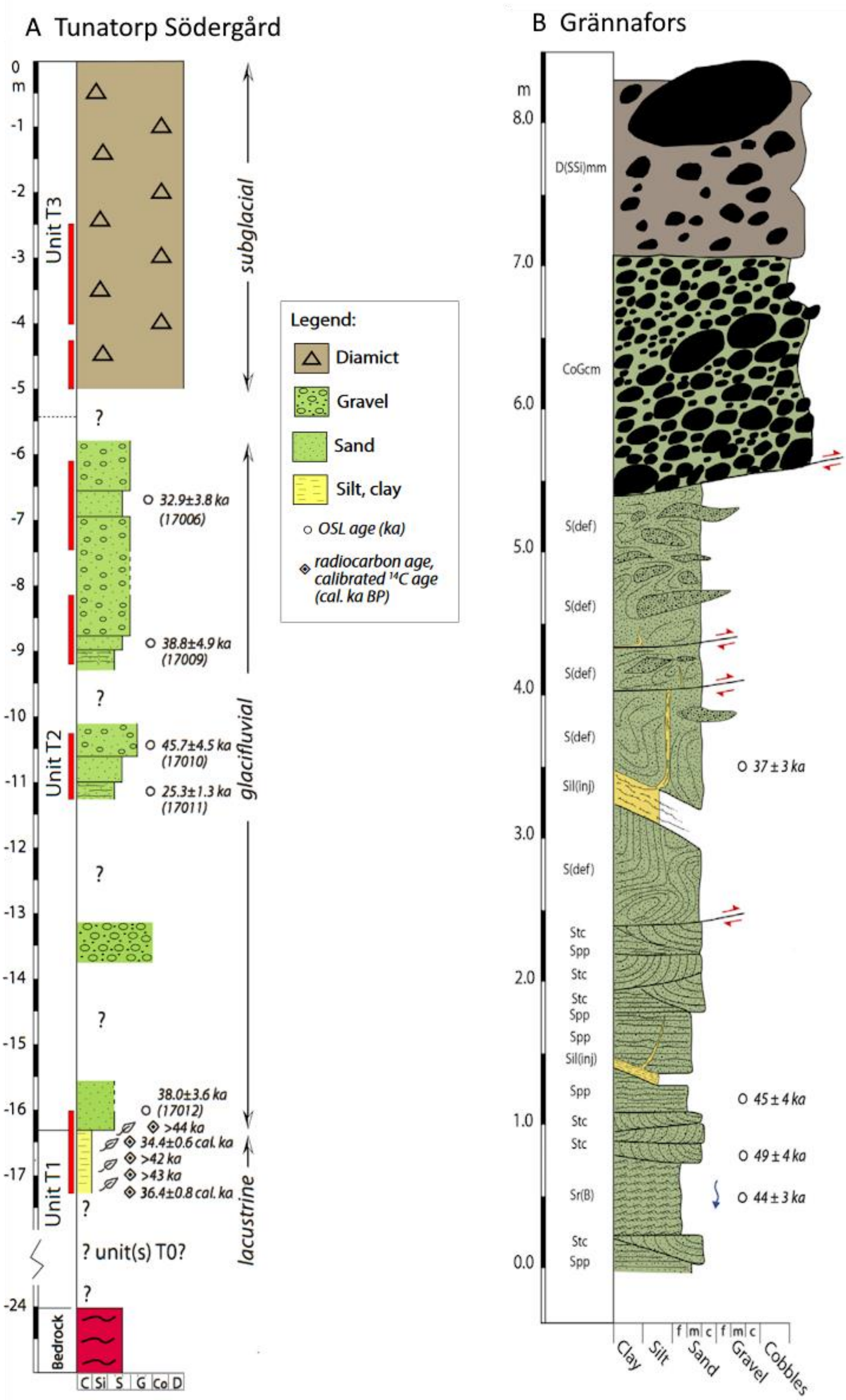

Appendix 7.C. Core logs from Möller and Murray (2015), showing the sampling sites of Nykulla (A) and Klockaregården (B).

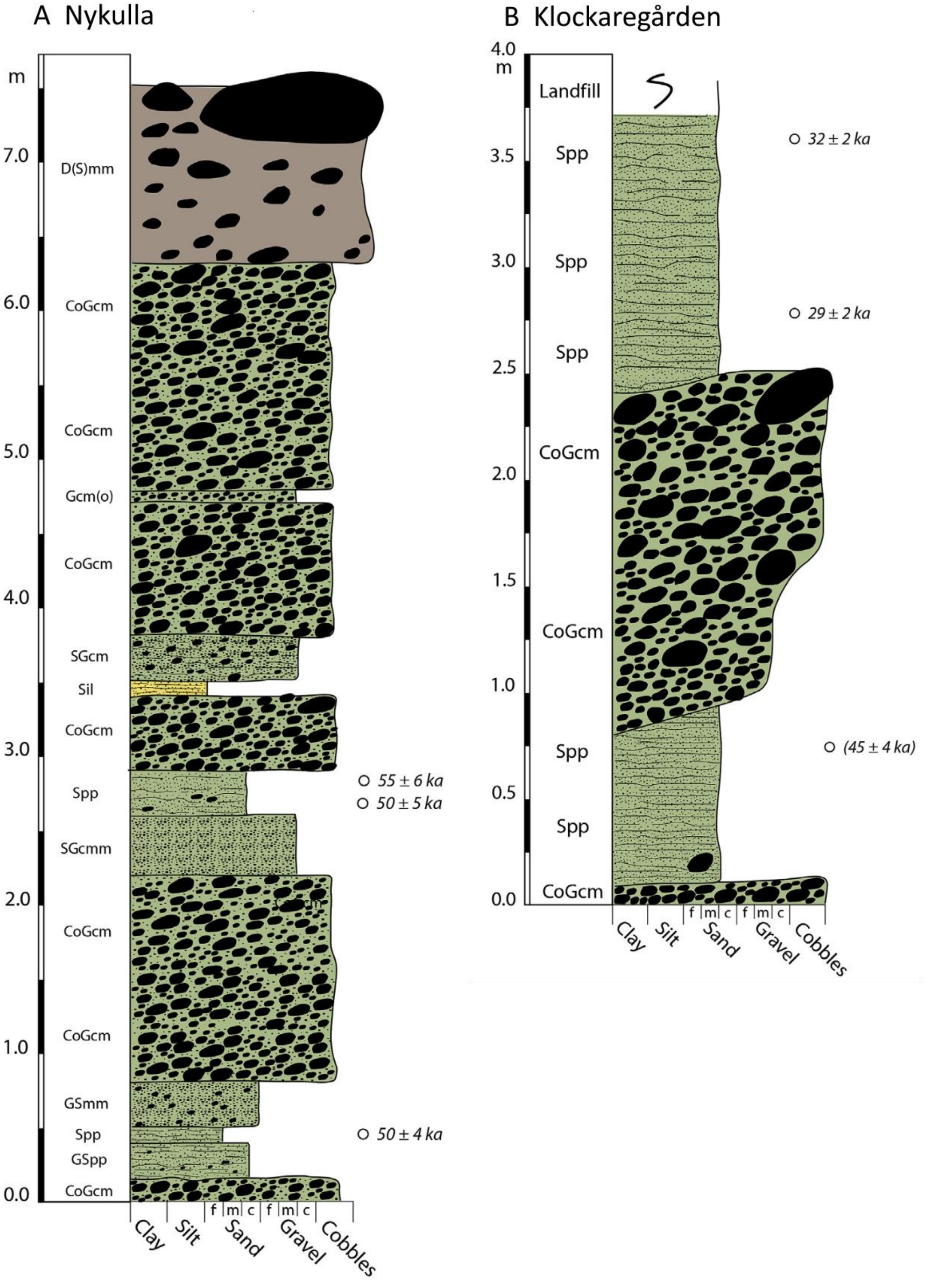

References

Gandahl, R. (1952). Bestämning av kornstorlek med hydrometer. Rapport 22 from Statens Väginstitut Stockholm. *Geologiska Föreningens Förhandlingar 1952;74 (4)*: 1-16.